Electromagnetic form factor of baryons from Chiral Effective field theory

Lingyun Dai

(Hunan university)

with J.Haldenbauer and U.-G. Meissner

Based on: JHEP1707 (2017) 078; PRD96 (2017) 116001; PRD98 (2018) 014005;

Sep. 2019， Hefei

湖南大學
HUNAN UNIVERSITY

Outlines

1. Introduction
2. NN scattering amplitude
3. NN FSI： proton FF
4. $\Lambda_c\Lambda_c$ FSI： Λ_c FF
5. Summary

1. Introduction

- Nucleon anti-nucleon: one of the most typical strong interactions
- **LEAR** has done lots of measurements

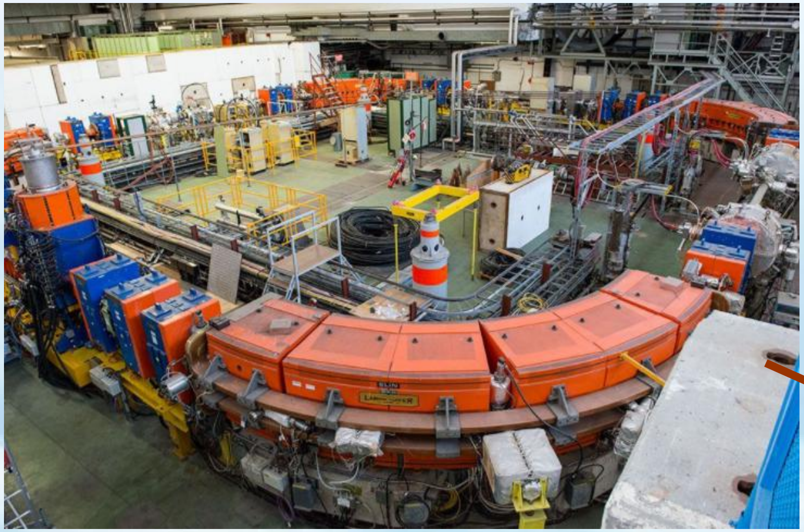

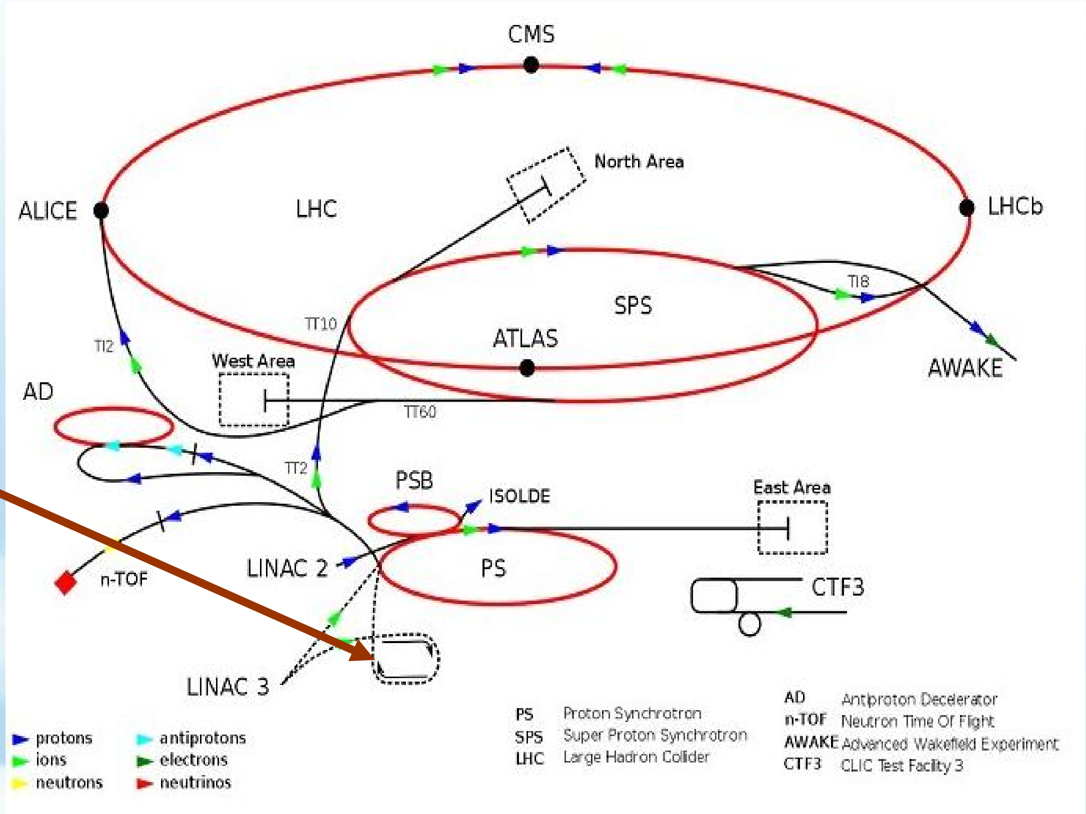

Baryon anti-baryon spectrum

- Threshold enhancement of baryon anti-baryon is observed by lots of experiment: pp, ΛΛ, ΣΣ, $\Lambda_c\Lambda_c$, ΞΞ(?)...
- Their interactions are important to study the the structures in the baryon anti-baryon spectroscopy.
- BABAR, BESIII, BelleII...
- FAIR: PANDA (pp), PAX (polarized p)?

red: anti-baryon

Strategy

- New insights in strong interactions?

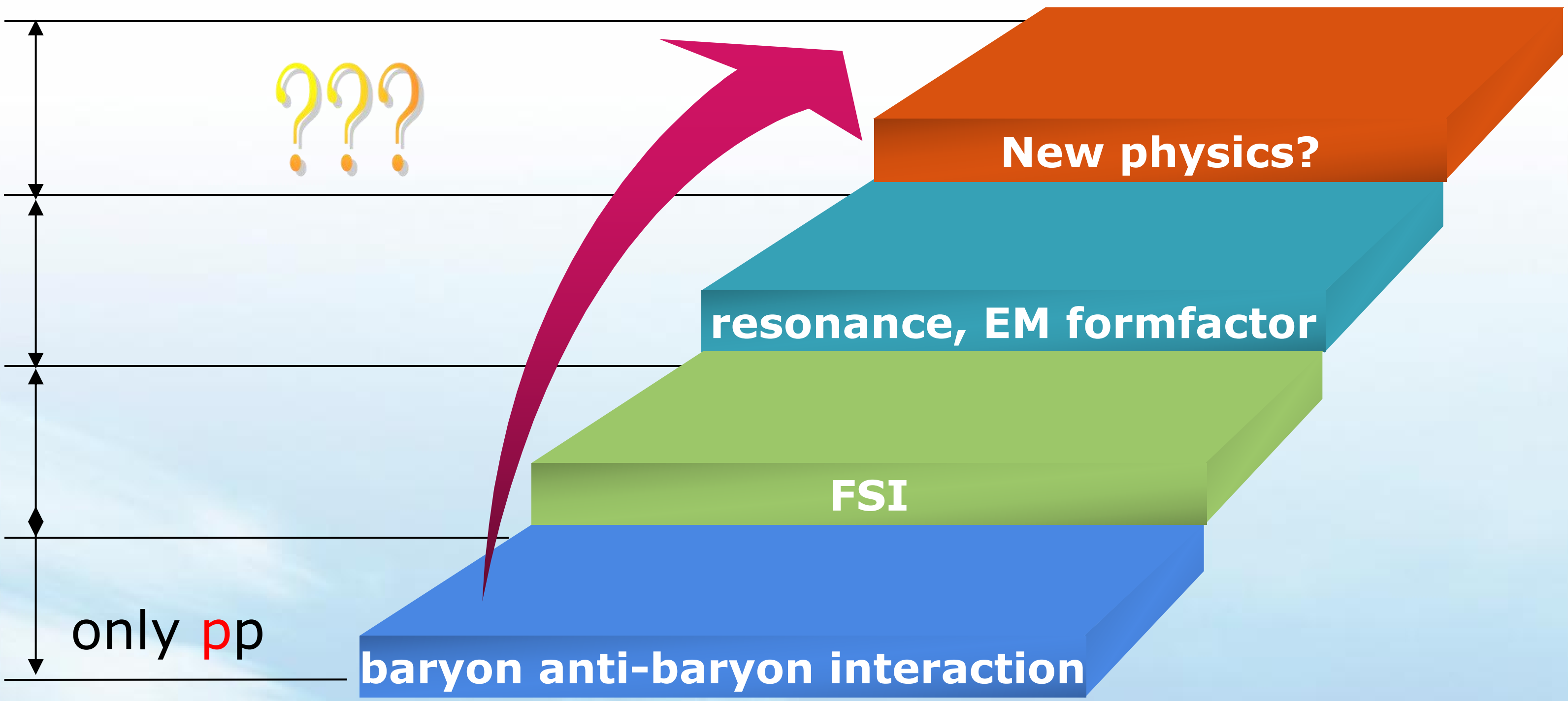

2. NN scattering amplitudes

- **NN scattering amplitude, two parts**
  - elastic NN scattering:
    - pion(s) exchange: NN Chiral EFT+G-parity
    - LECs of contact term: to be fixed by data
  - annihilation: unitarity, fit to the data

E.Epelbaum *et.al.*, EPJA51 (2015) , 53

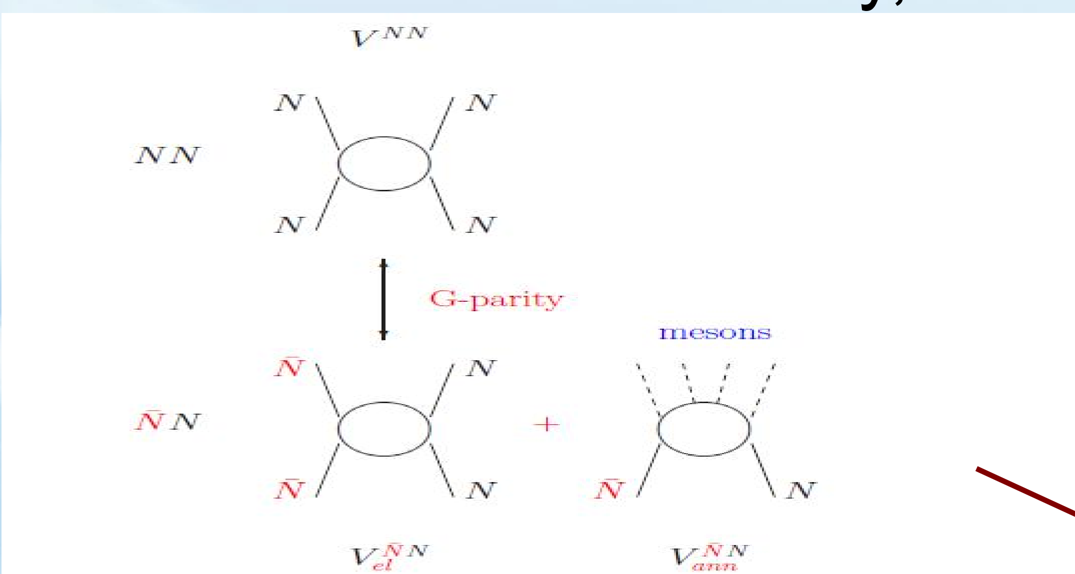

$$
\begin{aligned}
V^{NN} &= \quad V_{1\pi} + V_{2\pi} + V_{3\pi} + \ldots + V_{cont} \\
V^{\bar{N}N}_{el} &= -V_{1\pi} + V_{2\pi} - V_{3\pi} + \ldots + V_{cont} \\
V^{\bar{N}N}_{ann} &= \sum\nolimits_X V^{\bar{N}N \to X}
\end{aligned}
$$

J.Haidenbauer, talk at Bochum

ChEFT

- Up to N^{3}LO, in time ordered ChEFT:
  - only irreducible diagrams contributes
  - Lippmann-Shwinger equation

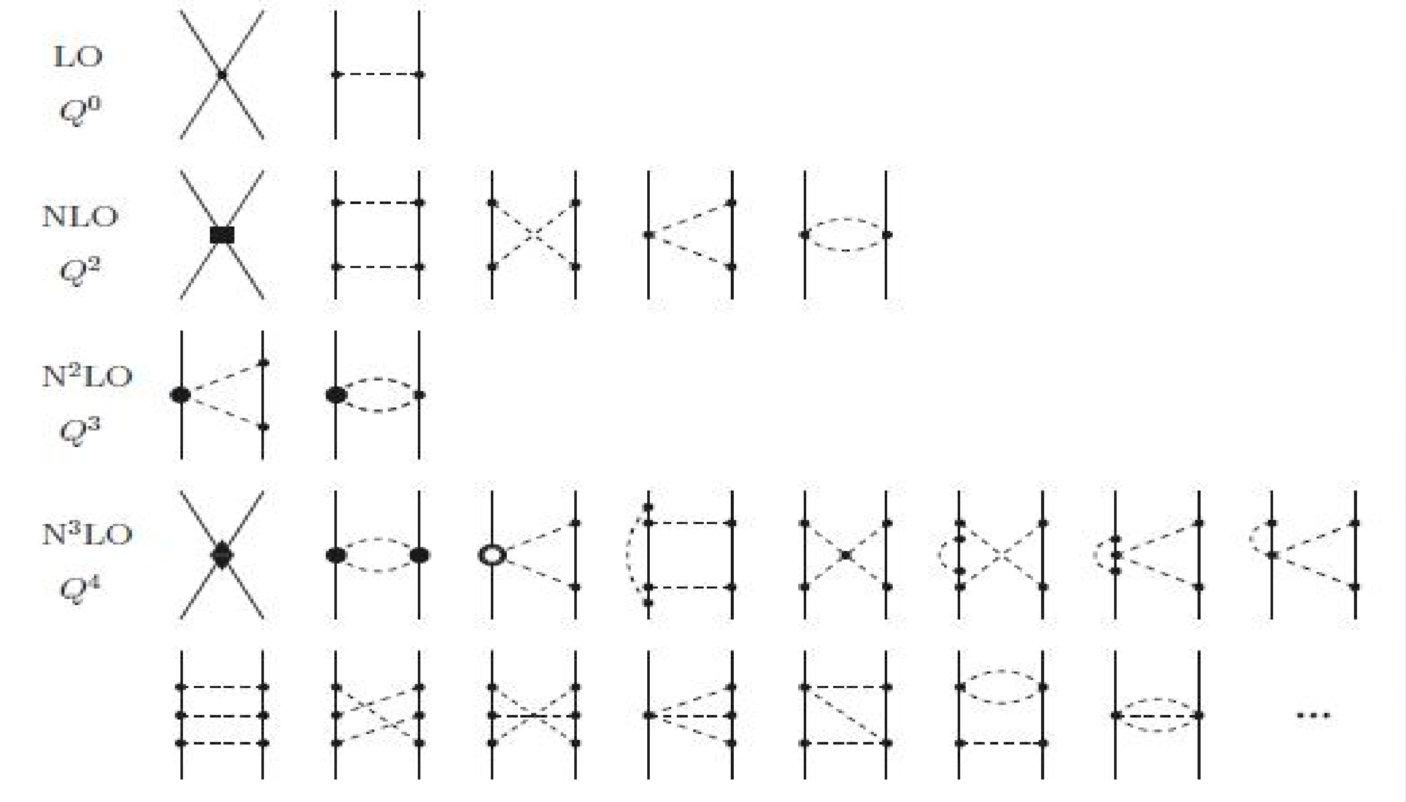

ChEFT: potentials

- pion(s) exchange potentials:

$$V_{1\pi}(q) = \left(\frac{g_A}{2F_\pi}\right)^2 \left(1 - \frac{p^2 + p'^2}{2m^2}\right) \boldsymbol{\tau}_1 \cdot \boldsymbol{\tau}_2 \frac{\boldsymbol{\sigma}_1 \cdot \mathbf{q}\, \boldsymbol{\sigma}_2 \cdot \mathbf{q}}{\mathbf{q}^2 + M_\pi^2}$$

$$\begin{aligned} V_{2\pi} &= V_C + \boldsymbol{\tau}_1 \cdot \boldsymbol{\tau}_2 W_C + [V_S + \boldsymbol{\tau}_1 \cdot \boldsymbol{\tau}_2 W_S]\, \boldsymbol{\sigma}_1 \cdot \boldsymbol{\sigma}_2 + [V_T + \boldsymbol{\tau}_1 \cdot \boldsymbol{\tau}_2 W_T]\, \boldsymbol{\sigma}_1 \cdot \boldsymbol{q}\, \boldsymbol{\sigma}_2 \cdot \boldsymbol{q} \\ &+ [V_{LS} + \boldsymbol{\tau}_1 \cdot \boldsymbol{\tau}_2 W_{LS}]\, i(\boldsymbol{\sigma}_1 + \boldsymbol{\sigma}_2) \cdot (\boldsymbol{q} \times \boldsymbol{k}) , \end{aligned}$$

- Fourier transformation: change it into corordinat space to do regularization

$$V_C(q) = 4\pi \int_0^\infty f(r)\, V_C(r) j_0(qr) r^2 dr ,$$

$$V_S(q) = 4\pi \int_0^\infty f(r) \left(V_S(r) j_0(qr) + \tilde{V}_T(r) j_2(qr)\right) r^2 dr ,$$

$$V_T(q) = -\frac{12\pi}{q^2} \int_0^\infty f(r)\, \tilde{V}_T(r) j_2(qr) r^2 dr ,$$

$$V_{SL}(q) = \frac{4\pi}{q} \int_0^\infty f(r)\, V_{LS}(r) j_1(qr) r^3 dr .$$

$$f(r) = \left[1 - \exp\left(-\frac{r^2}{R^2}\right)\right]^n .$$

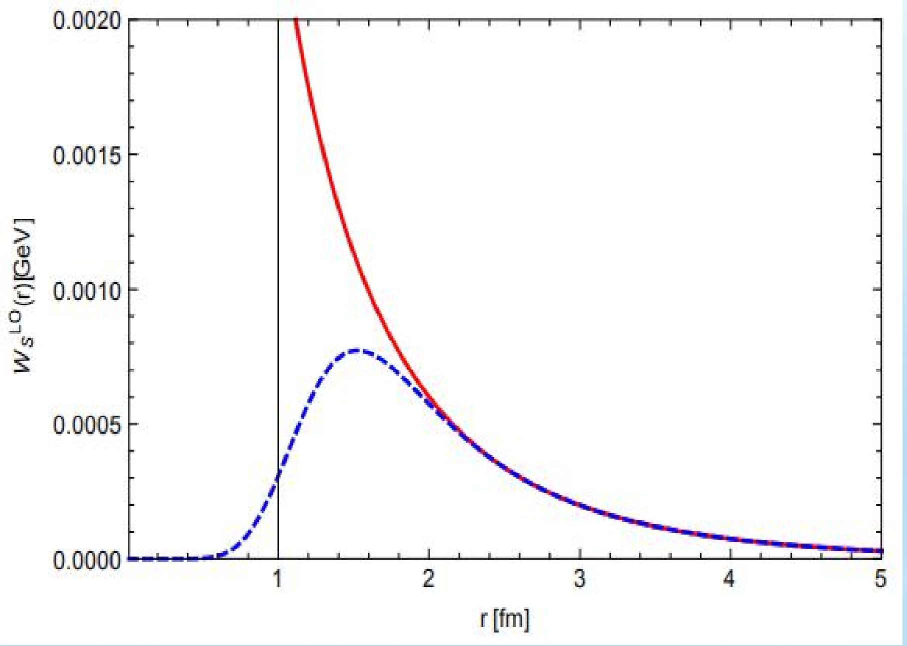

ChEFT: potentials

- Contact terms: short distance

$$
\begin{aligned}
V(^1S_0) &= \tilde{C}_{^1S_0} + C_{^1S_0}(p^2 + p'^2) + D^1{}_{^1S_0} p^2 p'^2 + D^2{}_{^1S_0}(p^4 + p'^4)\,, \\
V(^3S_1) &= \tilde{C}_{^3S_1} + C_{^3S_1}(p^2 + p'^2) + D^1{}_{^3S_1} p^2 p'^2 + D^2{}_{^3S_1}(p^4 + p'^4)\,, \\
V(^1P_1) &= C_{^1P_1}\, p p' + D_{^1P_1}\, p p'(p^2 + p'^2)\,, \\
V(^3P_1) &= C_{^3P_1}\, p p' + D_{^3P_1}\, p p'(p^2 + p'^2)\,, \\
V(^3P_0) &= C_{^3P_0}\, p p' + D_{^3P_0}\, p p'(p^2 + p'^2)\,, \\
V(^3P_2) &= C_{^3P_2}\, p p' + D_{^3P_2}\, p p'(p^2 + p'^2)\,, \\
V(^3D_1 - {}^3S_1) &= C_{\epsilon_1}\, p'^2 + D^1{}_{\epsilon_1} p^2 p'^2 + D^2{}_{\epsilon_1} p'^4\,, \\
V(^3S_1 - {}^3D_1) &= C_{\epsilon_1}\, p^2 + D^1{}_{\epsilon_1} p^2 p'^2 + D^2{}_{\epsilon_1} p^4\,,
\end{aligned}
$$

- Non-local regularization

$$
f(p', p) = \exp\left(-\frac{p'^m + p^m}{\Lambda^m}\right)
$$

- Annihilation terms: short distance physics, around 1 fm or less

$$
V_{\rm ann} = V_{\bar{N}N \to X} G_X V_{X \to \bar{N}N}
$$

the same form as that of contact terms

Ignore the transition between annihilation channels

ChEFT: potentials

- Imaginary term: -i, required by unitarity
- Real term: be absorbed into terms of momentum

$$
\begin{aligned}
V_{ann}^{L=0} &= -i\,(\tilde{C}^a_{^1S_0} + C^a_{^1S_0}p^2 + D^a_{^1S_0}p^4)(\tilde{C}^a_{^1S_0} + C^a_{^1S_0}p'^2 + D^a_{^1S_0}p'^4),\\
V_{ann}^{L=1} &= -i\,(C^a_{\alpha}p + D^a_{\alpha}p^3)(C^a_{\alpha}p' + D^a_{\alpha}p'^3),\\
V_{ann}^{L=2} &= -i\,(D^a_{\beta})^2p^2p'^2,\\
V_{ann}^{L=3} &= -i\,(D^a_{\gamma})^2p^3p'^3,
\end{aligned}
$$

$$
\begin{aligned}
V_{ann}^{S\to S} &= -i\,(\tilde{C}^a_{^3S_1} + C^a_{^3S_1}p^2 + D^a_{^3S_1}p^4)(\tilde{C}^a_{^3S_1} + C^a_{^3S_1}p'^2 + D^a_{^3S_1}p'^4),\\
V_{ann}^{S\to D} &= -i\,(\tilde{C}^a_{^3S_1} + C^a_{^3S_1}p^2D^a_{^3S_1}p^4)\,C^a_{\epsilon_1}p'^2,\\
V_{ann}^{D\to S} &= -i\,C^a_{\epsilon_1}p^2\,(\tilde{C}^a_{^3S_1} + C^a_{^3S_1}p'^2 + D^a_{^3S_1}p'^4),\\
V_{ann}^{D\to D} &= -i\,[(C^a_{\epsilon_1})^2 + (C^a_{^3D_1})^2]p^2p'^2\,.
\end{aligned}
$$

Expansion around NN threshold.
For 5π, 6π cases, they have small Brs.

- Higer power appears due to unitarity

Fits to Nijmegen's phase shifts

- PW projection, Lippmann-Shwinger equation

$$T_{L''L'}(p'',p';E_k) = V_{L''L'}(p'',p') + \sum_L \int_0^\infty \frac{dpp^2}{(2\pi)^3} V_{L''L}(p'',p) \frac{1}{2E_k - 2E_p + i0^+} T_{LL'}(p,p';E_k)$$

- The total χ^2 for different cutoffs

	R=0.7 fm	R=0.8 fm	R=0.9 fm	R=1.0 fm	R=1.1 fm	R=1.2 fm
$T_{\text{lab}} \leq 25$ MeV	0.002	0.003	0.004	0.004	0.019	0.036
$T_{\text{lab}} \leq 100$ MeV	0.032	0.023	0.025	0.036	0.090	0.176
$T_{\text{lab}} \leq 200$ MeV	0.143	0.106	0.115	0.177	0.312	0.626
$T_{\text{lab}} \leq 300$ MeV	2.855	2.012	2.171	3.383	5.531	9.479

- Cutoffs: 0.9, 1.0 fm, ChEFT does not work above k=500 MeV

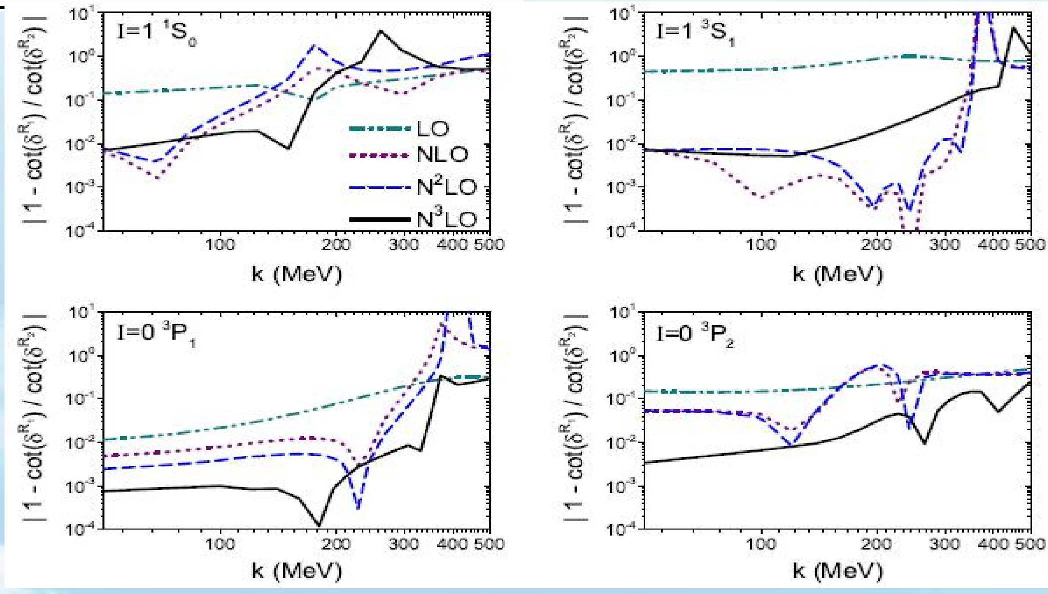

Phase shifts of different cutoff

- Lowest partial waves are perfect up to 300 MeV

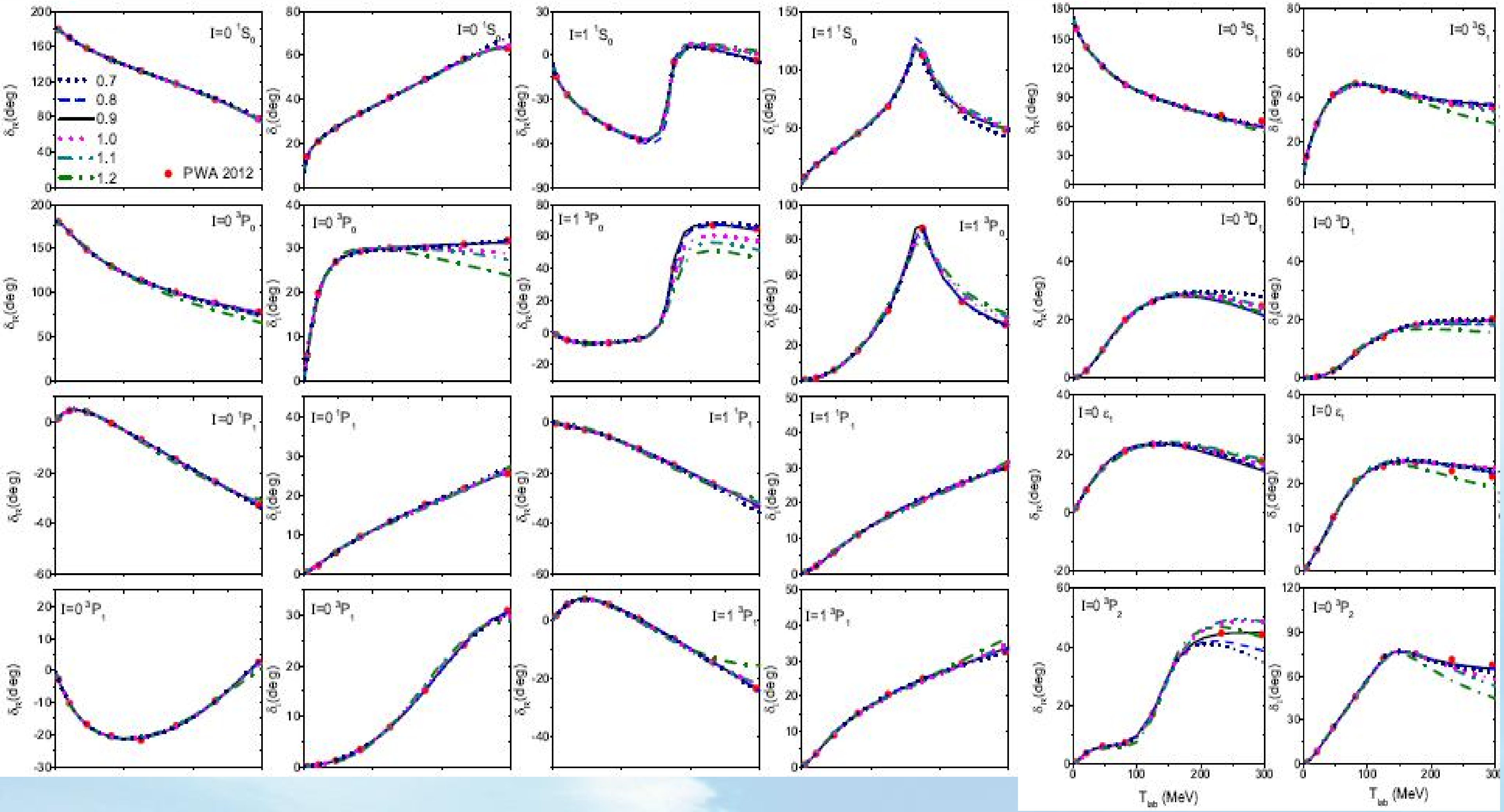

Phase shifts

- Higher partial waves may be worse above 200 MeV

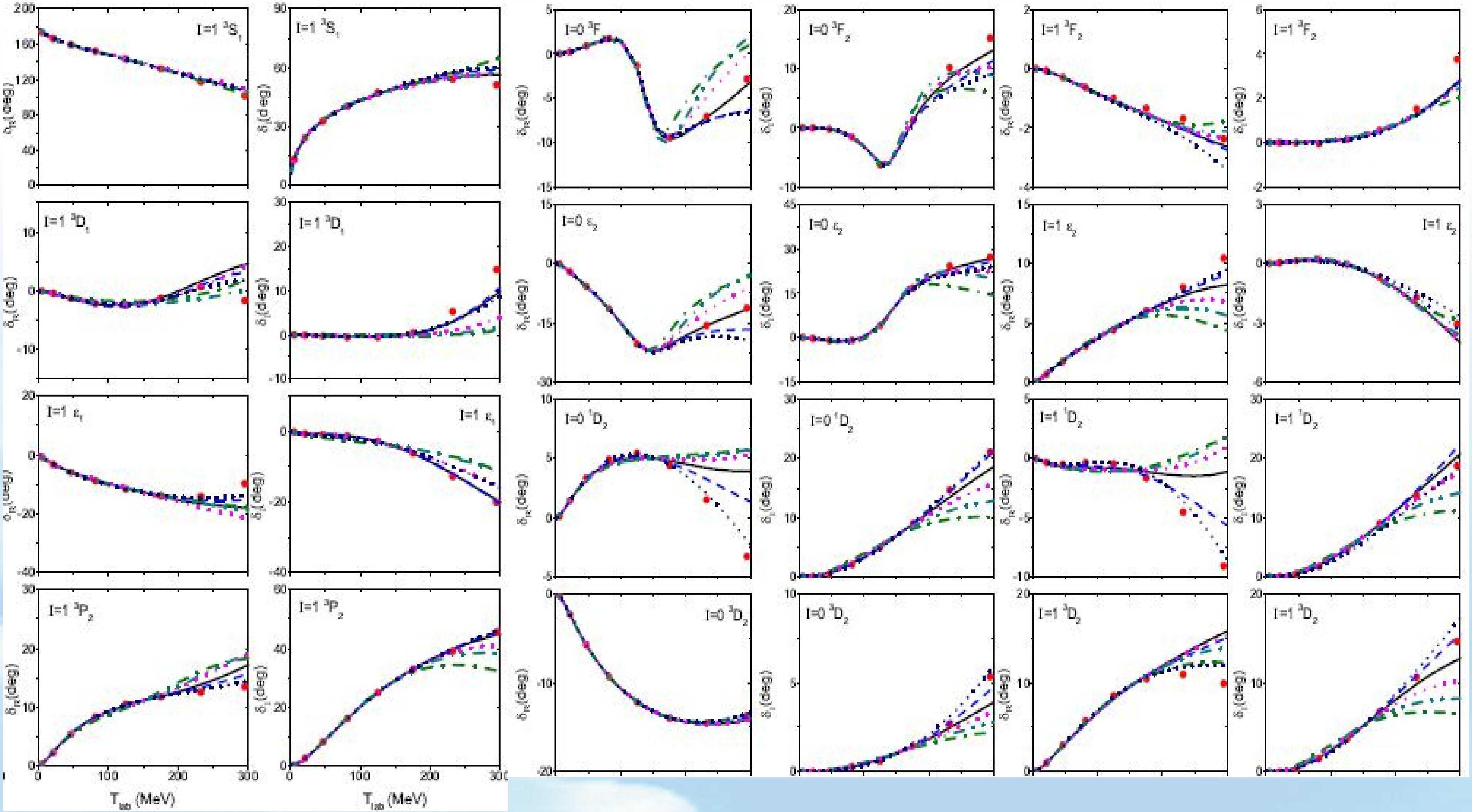

Error bands of different order

- Convergent when increasing orders, even in resonance region
- LO provides very limited description, only S-wave
- N^{3}LO,up to 300 MeV for S- and P- waves

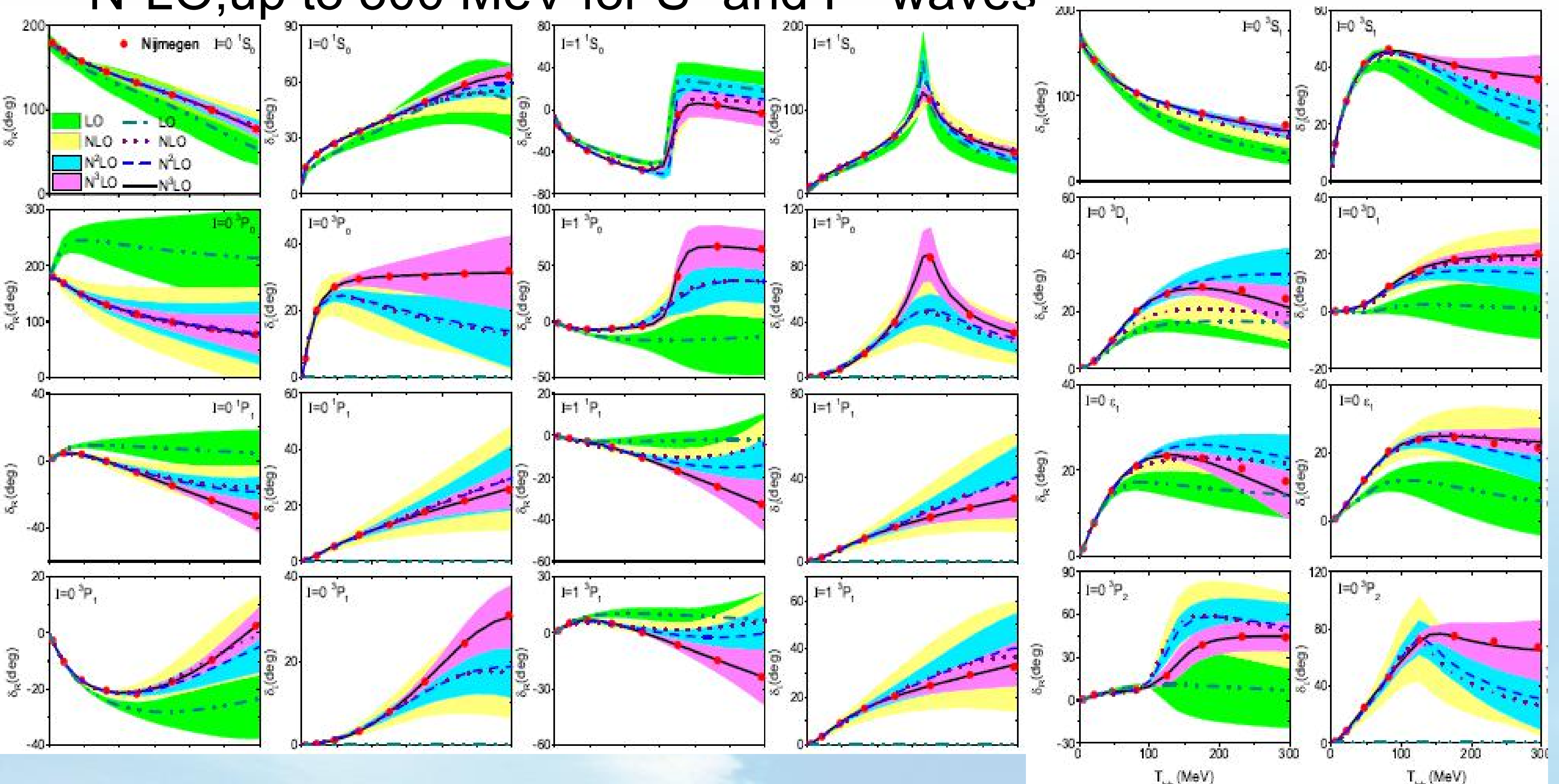

Error bands of different order

- Higher partial waves are well described at least up to 200 or 250 MeV

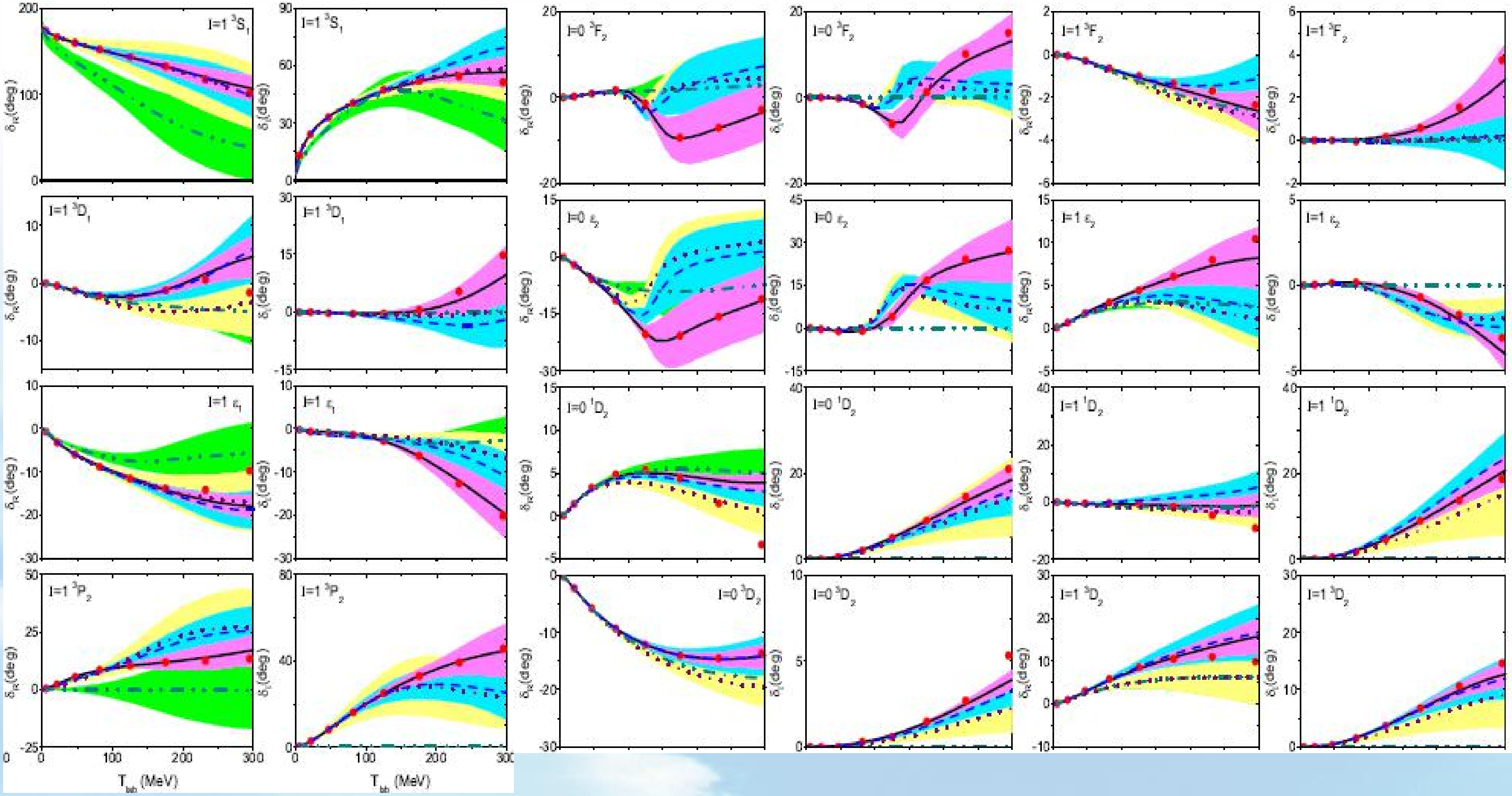

Observables

- Cross sections

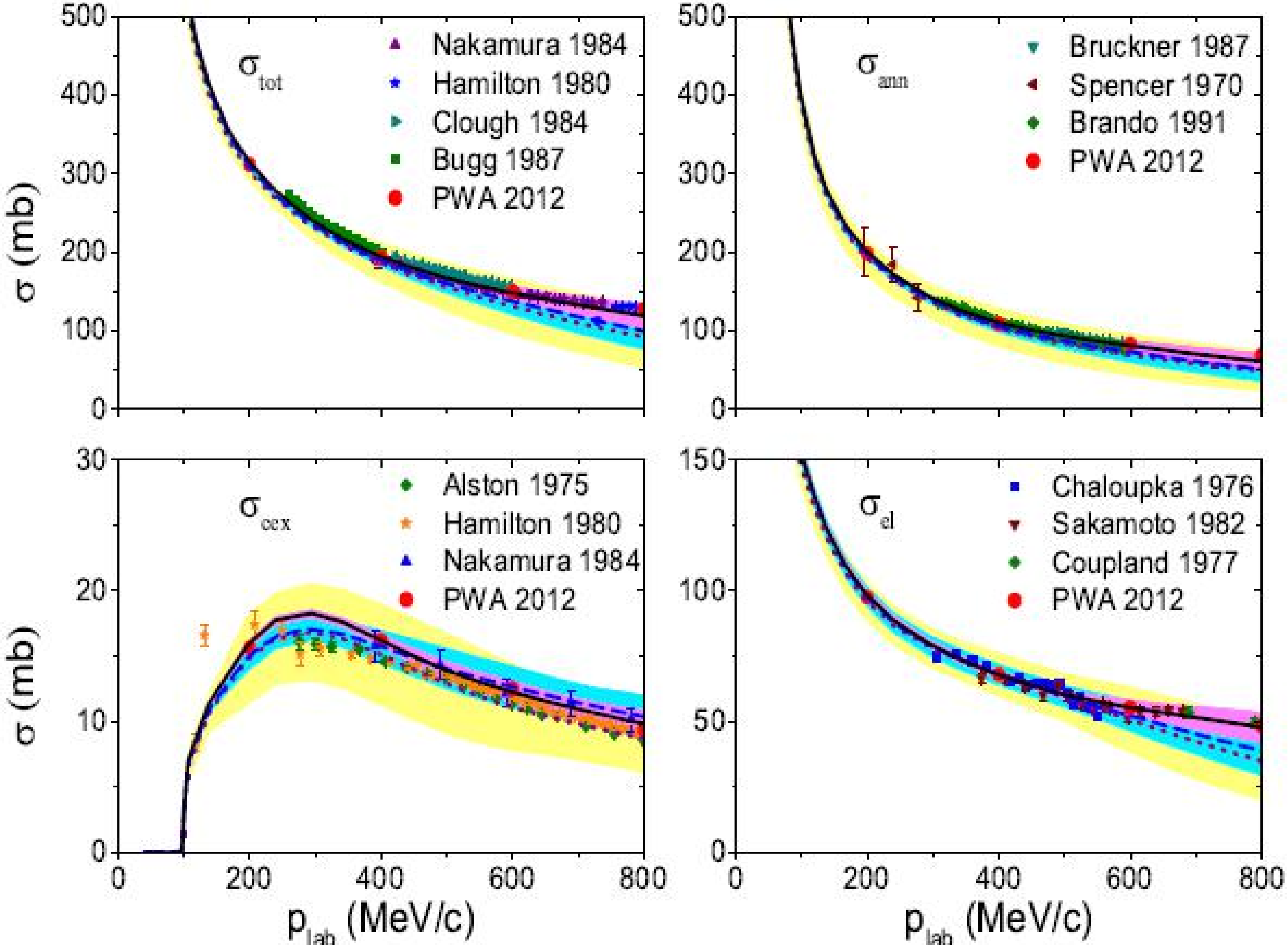

Angular distribution

- Differential cross section, analyzing power and correlation parameters are helpful for PWA

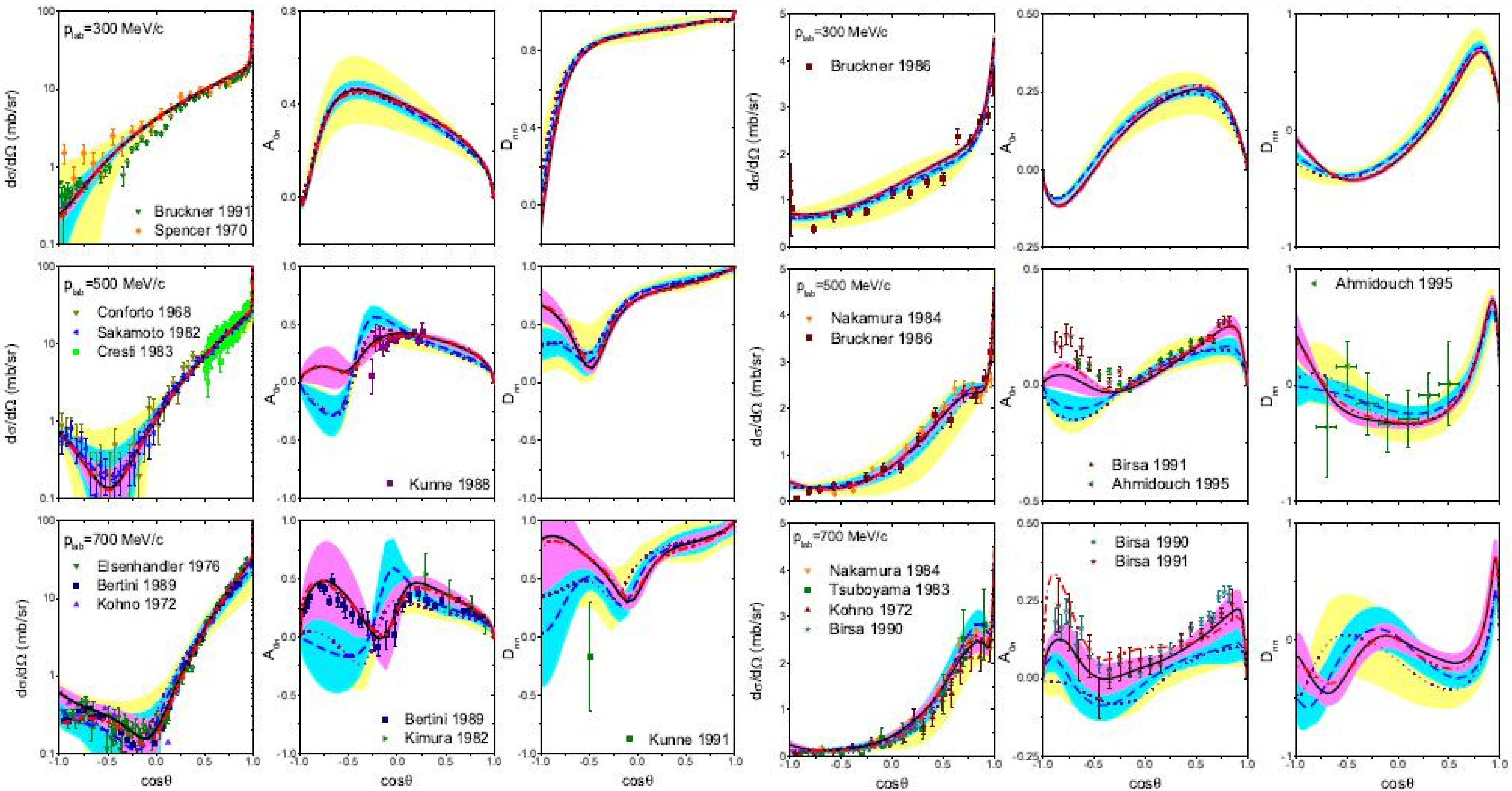

pp annihilation cross section

- Check in low energy region
- The 1/β² (not 1/β) anomalous threshold behaviour is caused by attractive Coulumn interaction

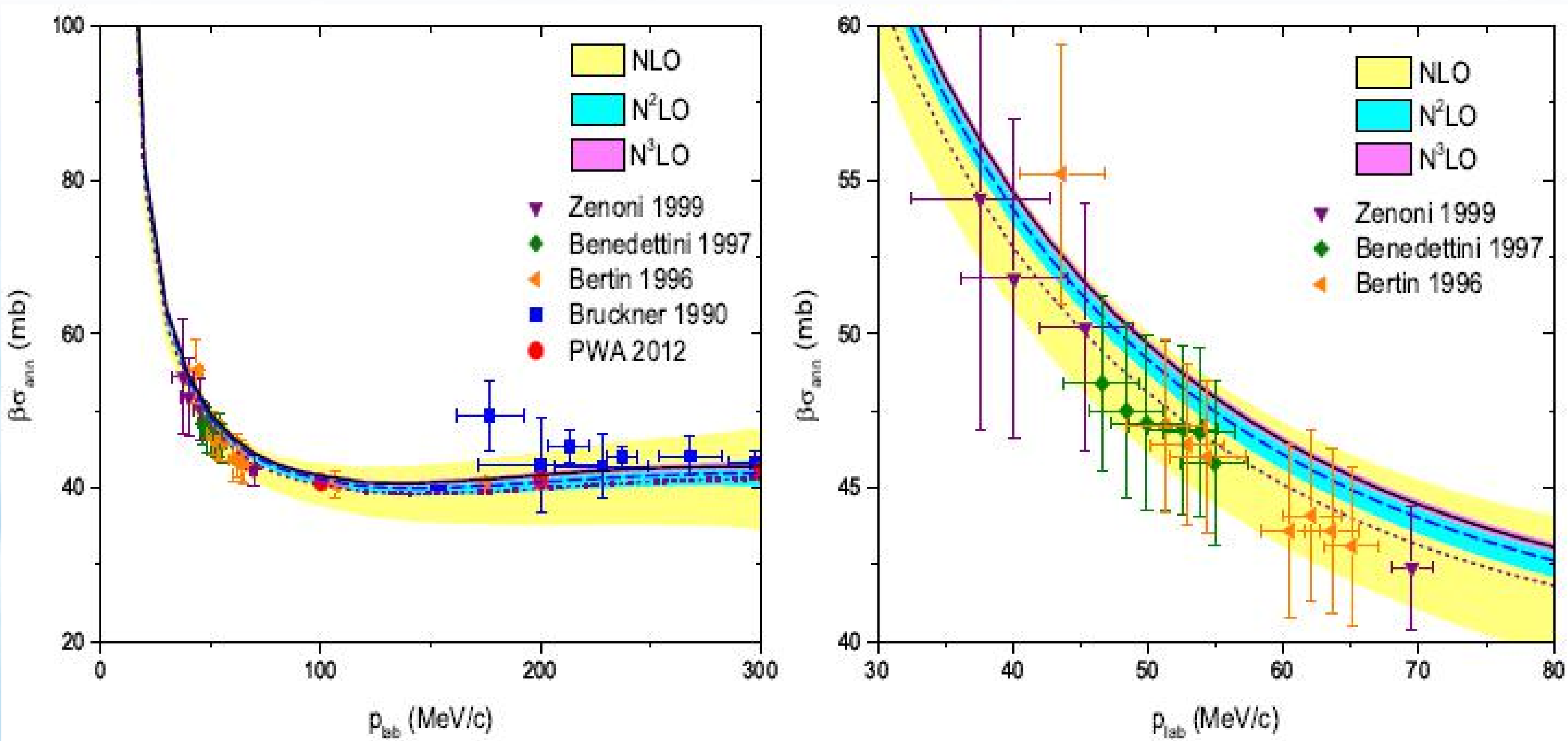

np annihilation cross section

- Purely isospin one components, helpful for PWA

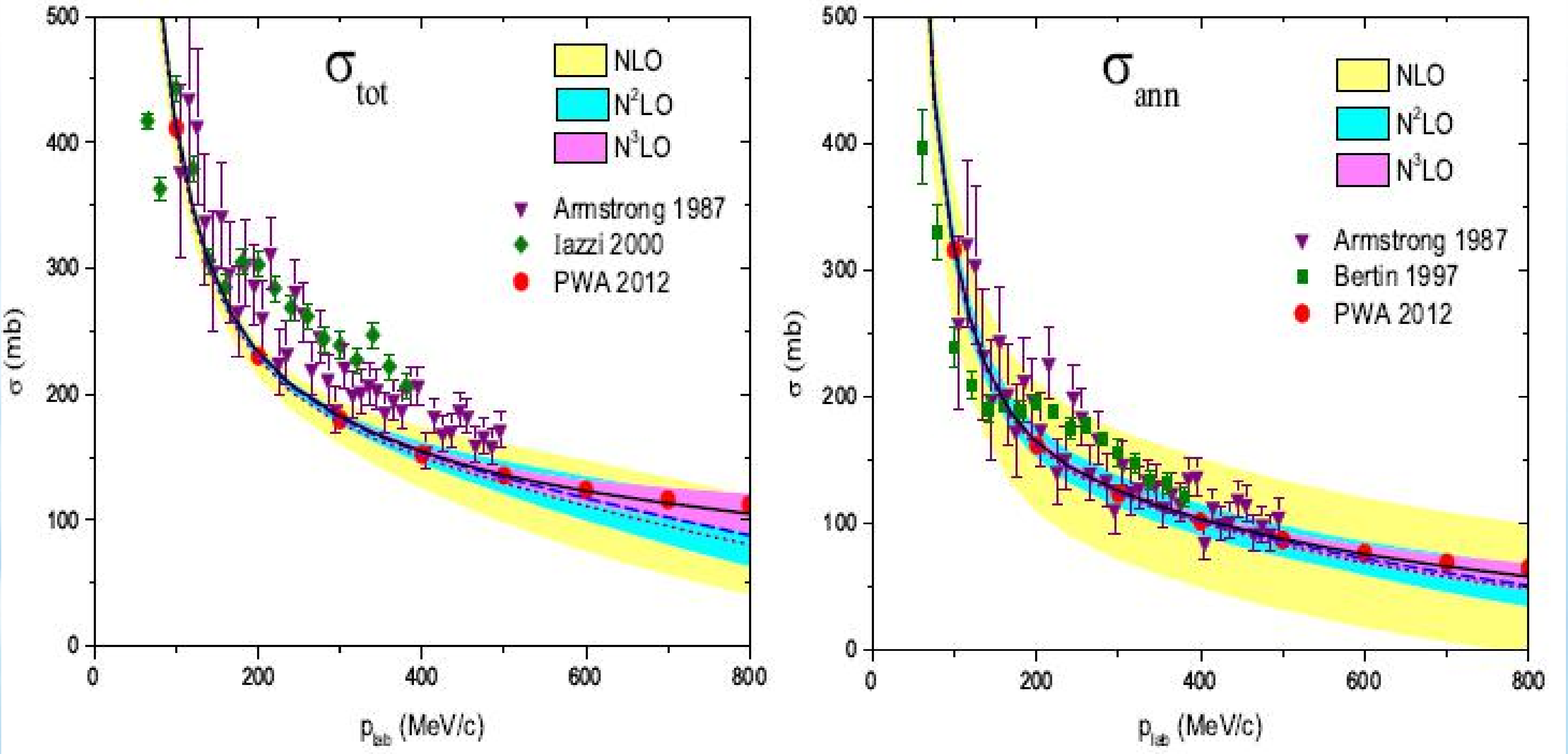

Energy shifts

- Hadronic shifts and broadenings in hyperfine states of pH
- Energy shifts and widths: Dese-Trueman formula

$$\Delta E_S + \mathrm{i}\,\frac{\Gamma_S}{2} = -\frac{4}{M_p r_B^3} a_S^{sc}\left(1 - \frac{a_S^{sc}}{r_B}\beta\right)$$

$$\Delta E_P + \mathrm{i}\,\frac{\Gamma_P}{2} = -\frac{3}{8 M_p r_B^5} a_P^{sc}$$

T.L. Trueman, NP26 (1961) 57
J. Carbonell *et.al.*, ZPA 343 (1992) 325

X.W. Kang *et.al. JHEP1402 (2014) 113*

	NLO	N^2LO	N^3LO	N^2LO [42]	Experiment
$E_{^1S_0}$ (eV)	−448	−446	−443	−436	−440(75) [98]
					−740(150) [97]
$\Gamma_{^1S_0}$ (eV)	1155	1183	1171	1174	1200(250) [98]
					1600(400) [97]
$E_{^3S_1}$ (eV)	−742	−766	−770	−756	−785(35) [98]
					−850(42) [99]
$\Gamma_{^3S_1}$ (eV)	1106	1136	1161	1120	940(80) [98]
					770(150) [99]
$E_{^3P_0}$ (meV)	17	12	8	16	139(28) [100]
$\Gamma_{^3P_0}$ (meV)	194	195	188	169	120(25) [100]
E_{1S} (eV)	−670	−688	−690	−676	−721(14) [98]
Γ_{1S} (eV)	1118	1148	1164	1134	1097(42) [98]
E_{2P} (meV)	1.3	2.8	4.7	2.3	15(20) [100]
Γ_{2P} (meV)	36.2	37.4	37.9	27	38.0(2.8) [100]

NN FSI：proton FF

- Proton form factor: probe of the inner structure of proton
- ee→pp, helpful for determine the space-like region FF

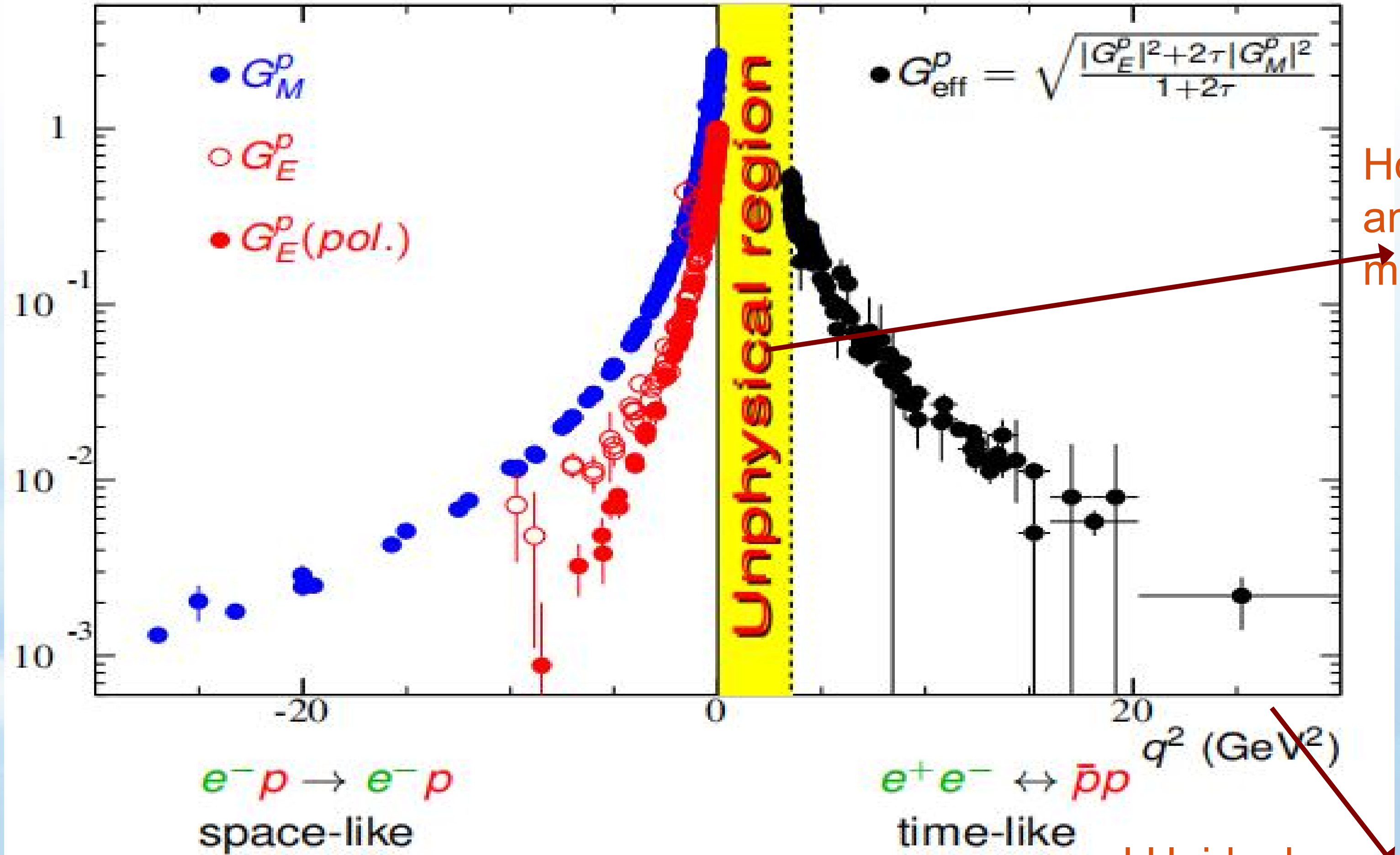

How to connect? amplitude analysis may help.

J.Haidenbauer, talk at Bochum

new measurement

- CMD-3 has excellent measurement in low energy region
- BESIII's in the region near threshold?

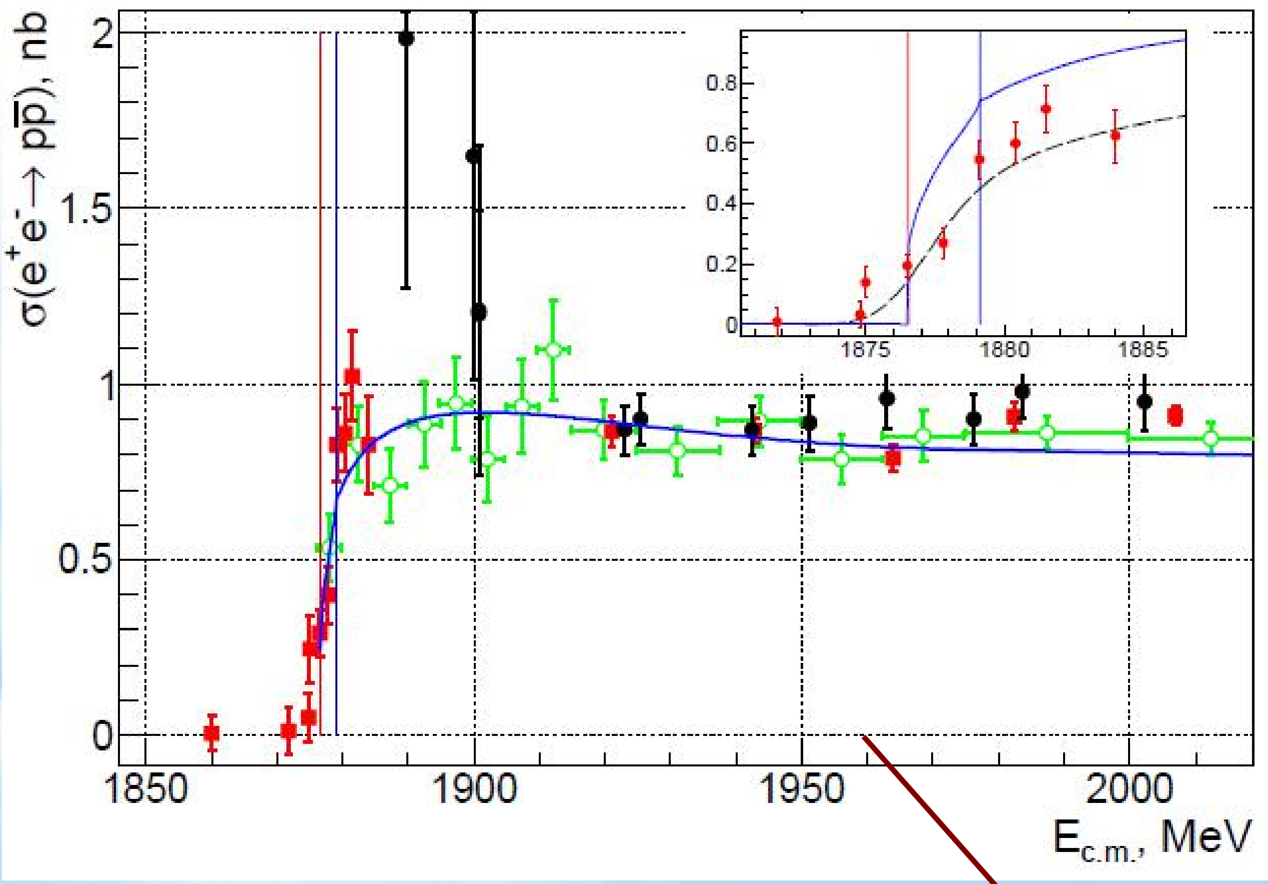

CMD-3, PLB05 (2019) 032

FSI

- To analyze ee→pp, we need to consider FSI
- Distorted-wave Born approximation (DWBA):

$$T_{\bar{N}N\to\bar{N}N} = V_{\bar{N}N\to\bar{N}N} + V_{\bar{N}N\to\bar{N}N}G_0T_{\bar{N}N\to\bar{N}N},$$
$$T_{e^+e^-\to\bar{N}N} = V_{e^+e^-\to\bar{N}N} + V_{e^+e^-\to\bar{N}N}G_0T_{\bar{N}N\to\bar{N}N},$$

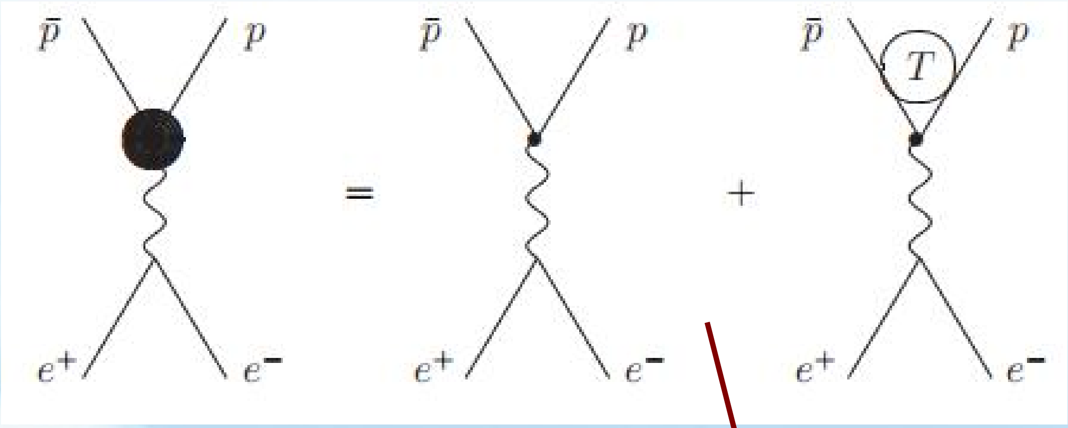

- Vector meson dominance: $^3S_1$-$^3D_1$

J.Haidenbauer, X.-W. Kang, U.-G. Meißner, NPA 929 (2014) , PRD91 (2015) 074003.

N^{2}LO

- N^{2}LO result. N^{3}LO's is coming

$$\sigma_{e^+e^- \to \bar{p}p} = \frac{4\pi\alpha^2\beta}{3s} C_p(s) \left[|G_M(s)|^2 + \frac{2M_p^2}{s} |G_E(s)|^2 \right]$$

$$|G_{\rm eff}(s)| = \sqrt{\frac{\sigma_{e^+e^- \to \bar{p}p}(s)}{\frac{4\pi\alpha^2\beta}{3s} C_p(s) \left[1 + \frac{2M_p^2}{s}\right]}}$$

J.Haidenbauer, X.-W. Kang, U.-G. Meißner, NPA 929 (2014)

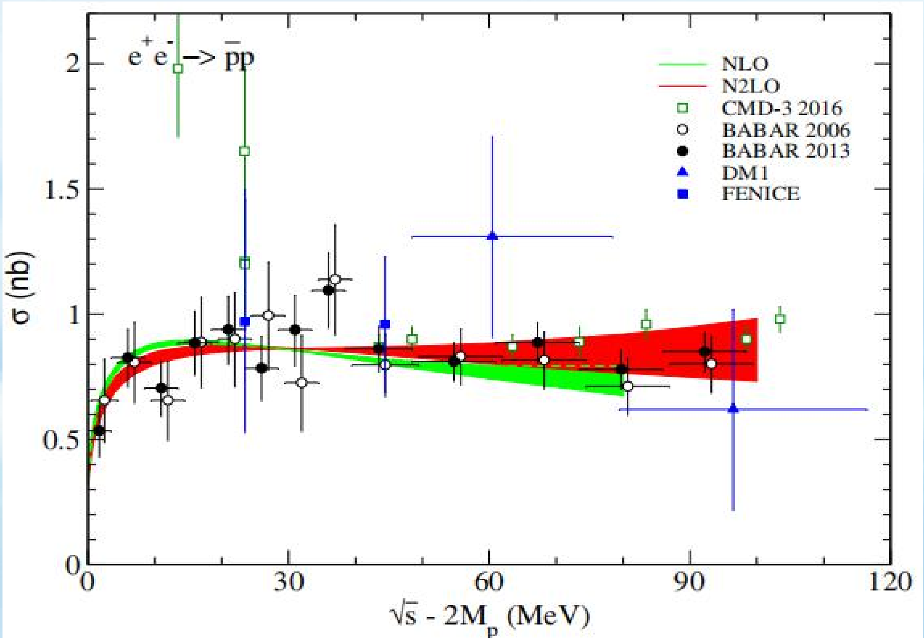

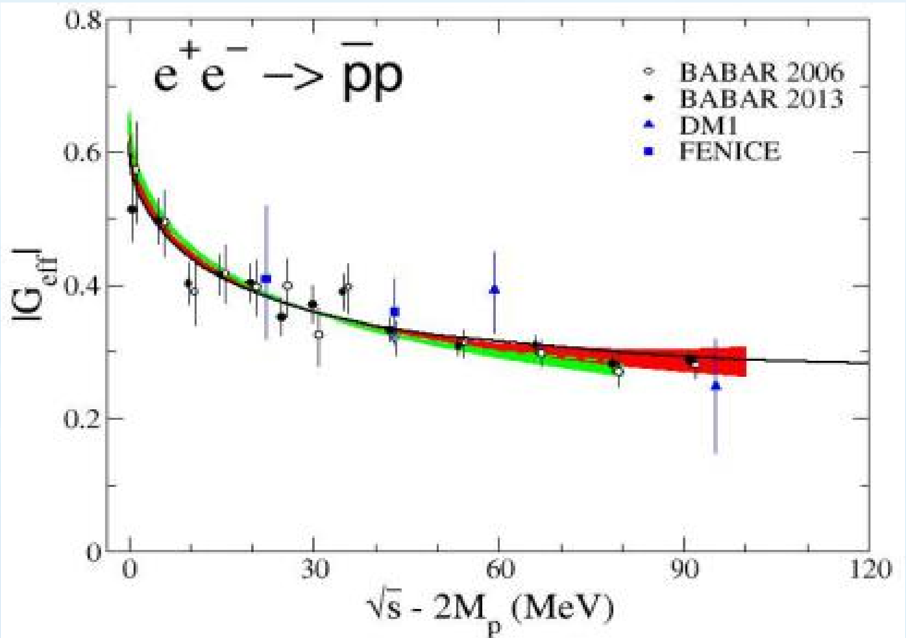

X1835?

- The amplitude gives information of structures, vice versa
- There is a structure around $p\bar{p}$ threshold in many channels

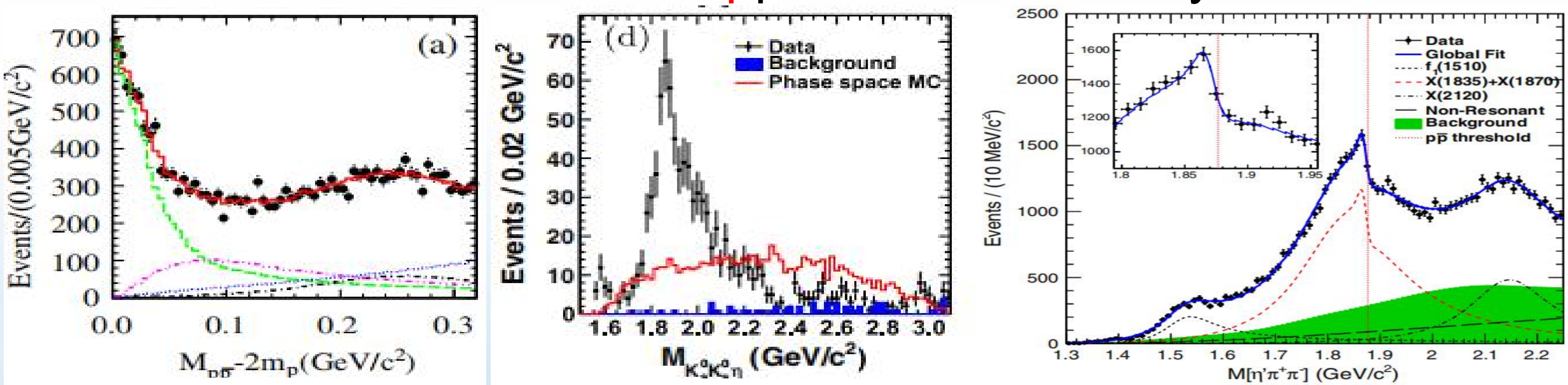

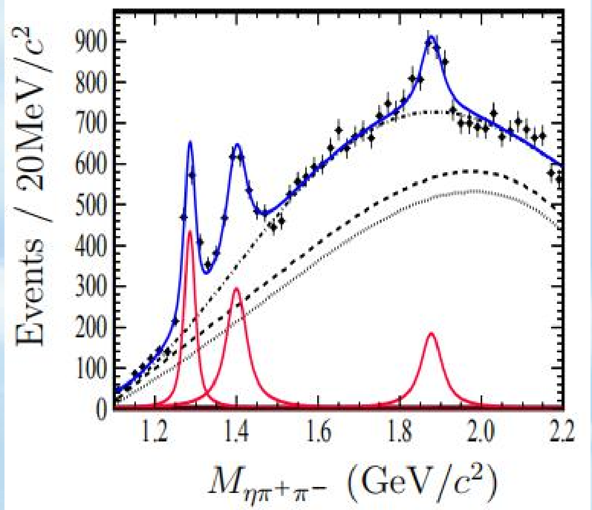

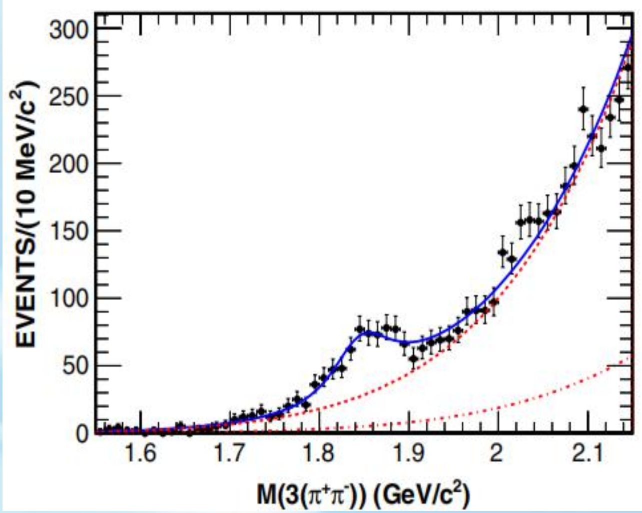

BESIII:
PRL108 (2016) 112003,
PRL115 (2015)091803,
PRL117 (2016)042002,
PRL107 (2011) 182001,
PRD88 (2013) 091502

DWBA

- The intermaediate states NN rescattering is included

$$J/\psi \to \gamma \bar{N}N \to \gamma \eta' \pi^+ \pi^-$$

- We need distorted-wave Born approximation (DWBA)

$$
\begin{aligned}
T_{\bar{N}N\to\bar{N}N} &= V_{\bar{N}N\to\bar{N}N} + V_{\bar{N}N\to\bar{N}N} G_0 T_{\bar{N}N\to\bar{N}N},\\
T_{\bar{N}N\to\eta'\pi\pi} &= V_{\bar{N}N\to\eta'\pi\pi} + T_{\bar{N}N\to\bar{N}N} G_0 V_{\bar{N}N\to\eta'\pi\pi},\\
A_{J/\psi\to\gamma\bar{N}N} &= A^0_{J/\psi\to\gamma\bar{N}N} + A^0_{J/\psi\to\gamma\bar{N}N} G_0 T_{\bar{N}N\to\bar{N}N},\\
A_{J/\psi\to\gamma\eta'\pi\pi} &= A^0_{J/\psi\to\gamma\eta'\pi\pi} + A^0_{J/\psi\to\gamma\bar{N}N} G_0 T_{\bar{N}N\to\eta'\pi\pi}\\
&= A^0_{J/\psi\to\gamma\eta'\pi\pi} + A_{J/\psi\to\gamma\bar{N}N} G_0 V_{\bar{N}N\to\eta'\pi\pi}.
\end{aligned}
$$

$BR(\bar{p}p \to \eta'\pi^+\pi^-) = 0.626\%$

X.W.Kang *et.al*., PRD91 (2015) 074003.

- J/ψ → ωpp, ϕpp channels: isospin 0 component does not contribute to the enhancement near the threshold

$$T_{\bar{p}p} = (T^{I=0} + T^{I=1})/2 \longrightarrow T = (0.4\,T^0 + 0.6\,T^1)$$

Modified isospin 1 NN amplitude

- Isospin 1 amplitude is modified slightly to fit to the J/ψ → γpp data
- Low energy part is the same as previous analysis
- After modification, we find a isospin 1 resonance: binding energy (-50.8-i 40.9) MeV, too wide to be seen

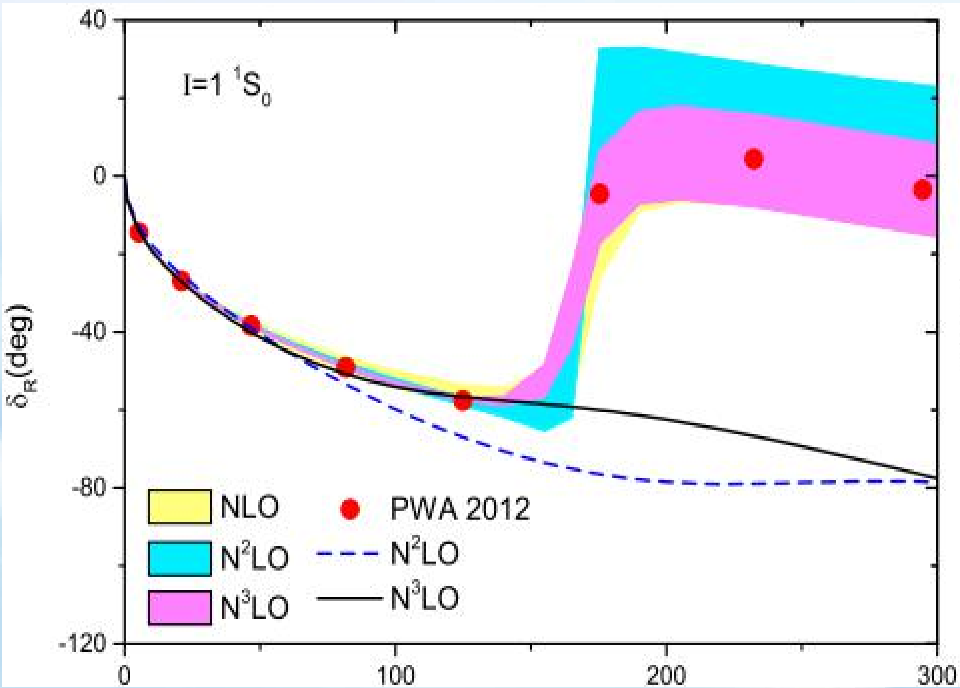

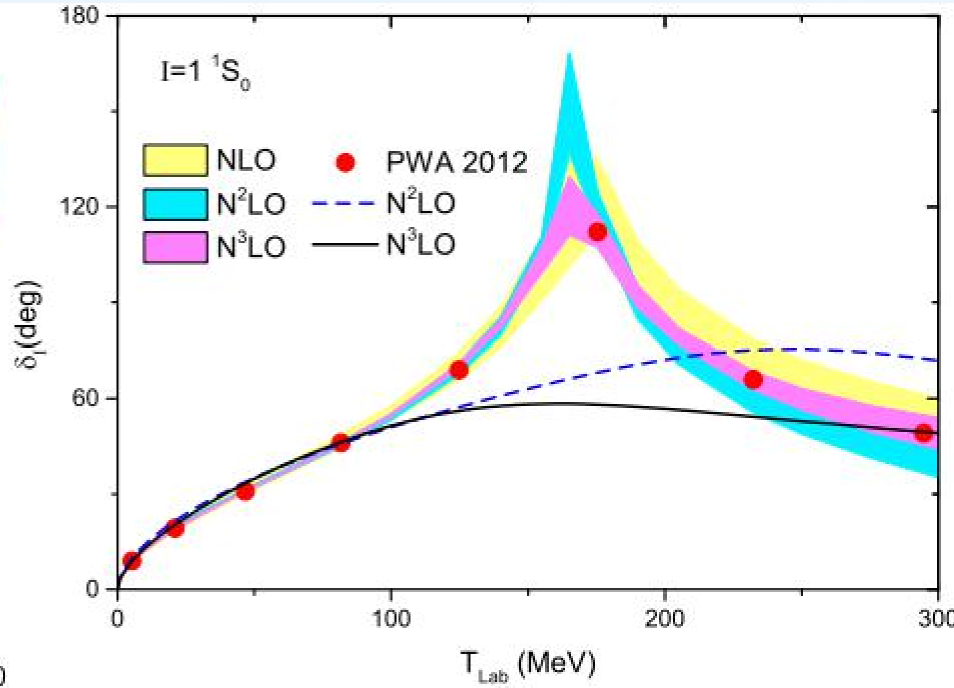

Threshold effects

- The inteference between background and cusp constructs the structre around pp threshold
- Bound state description is not necessary

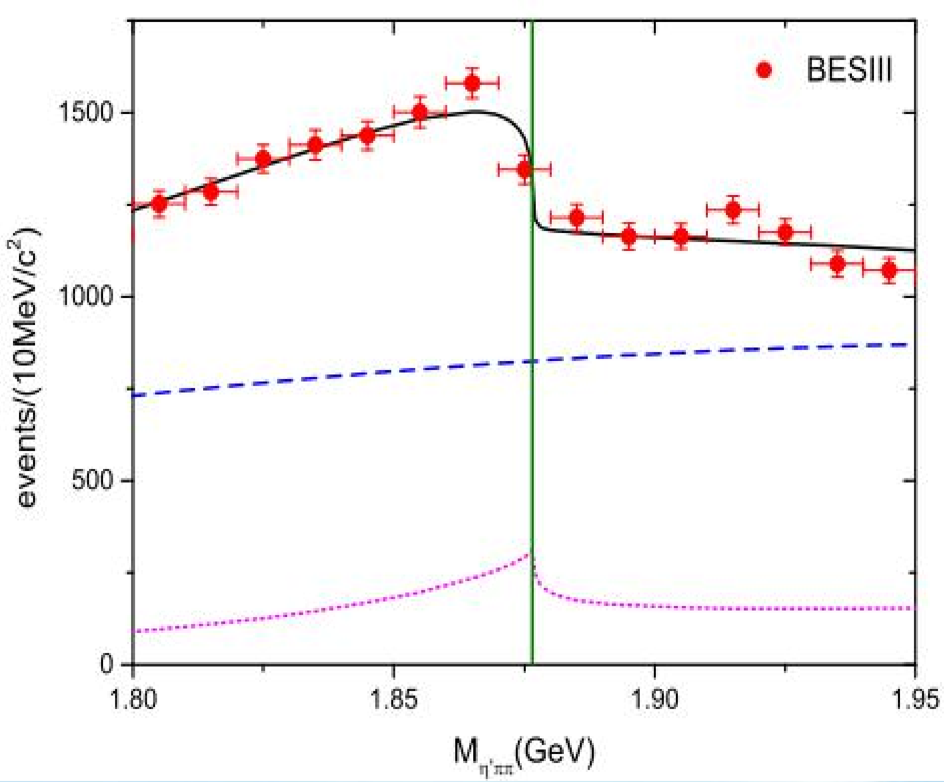

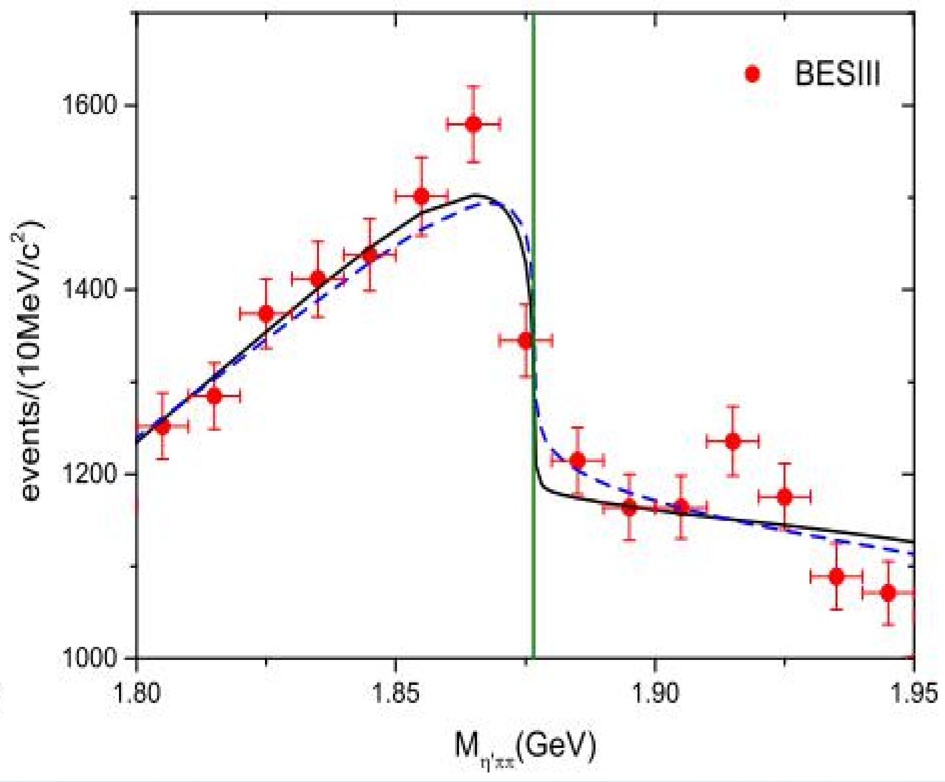

Prediction

- We suggest BESIII to study the process of $J/\psi \to \gamma\omega\rho^0$
- More narrow bound state has more pronouned structure

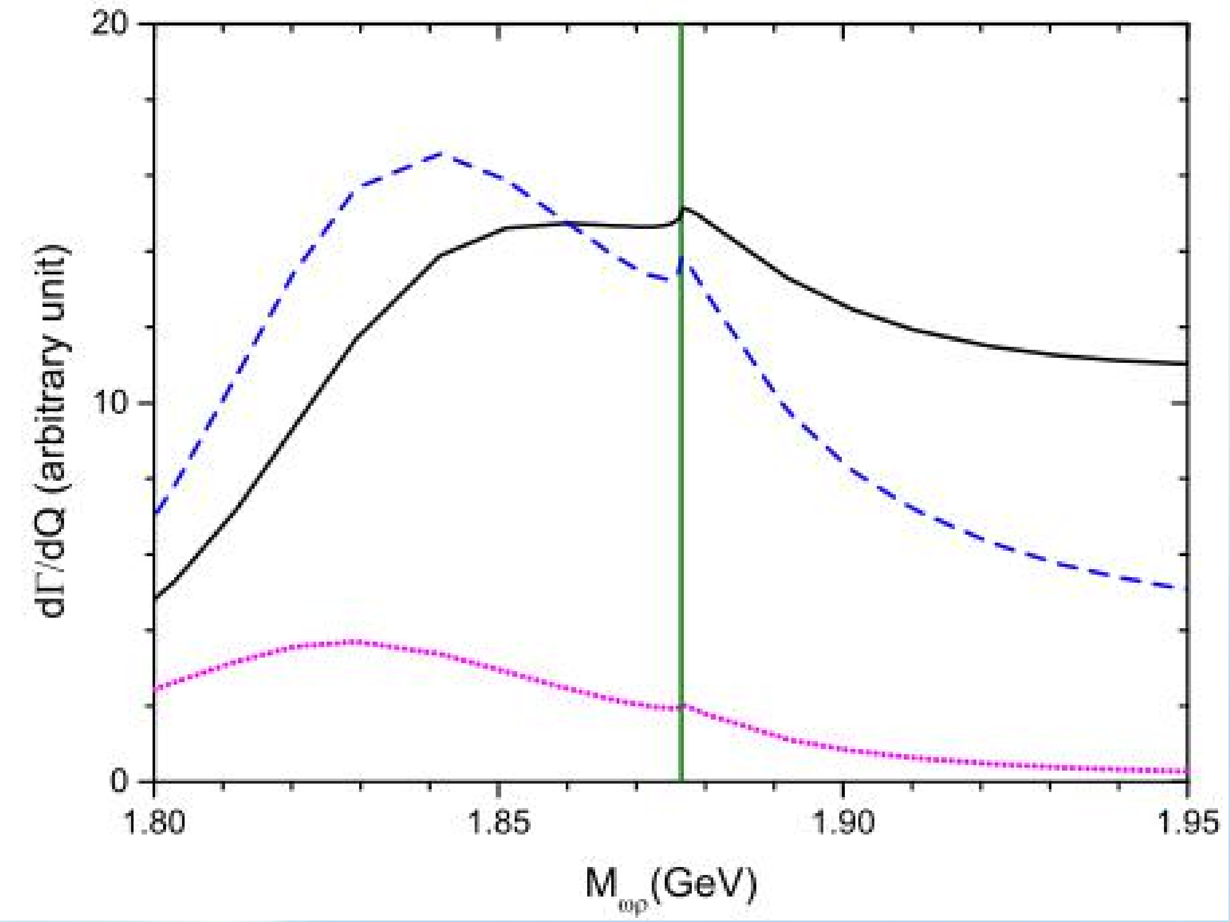

4. $\Lambda_c\Lambda_c$ FSI: Λ_c FF

- We need to clarify the resonances appear in $\Lambda_c\Lambda_c$ scattering amplitude
- With FSI we study ee→$\Lambda_c\Lambda_c$

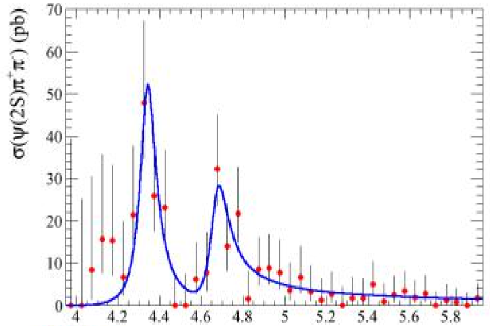

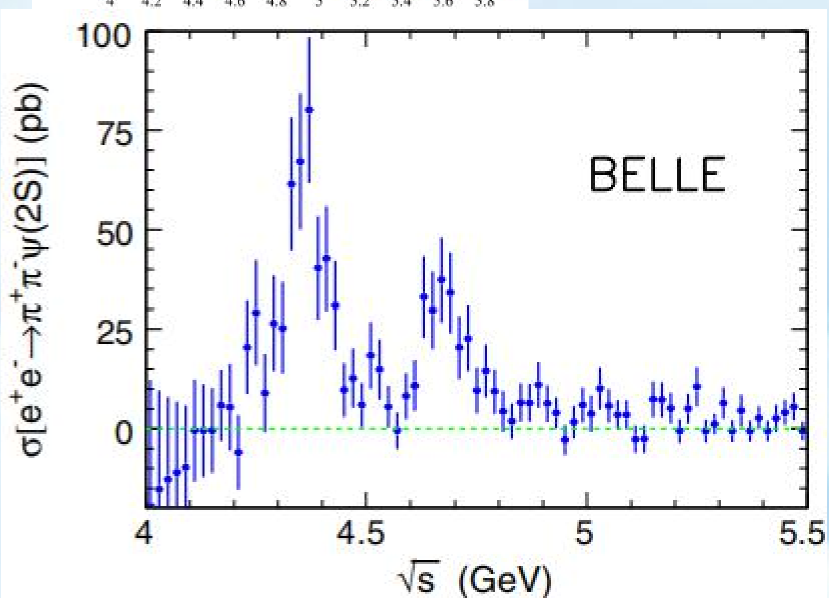

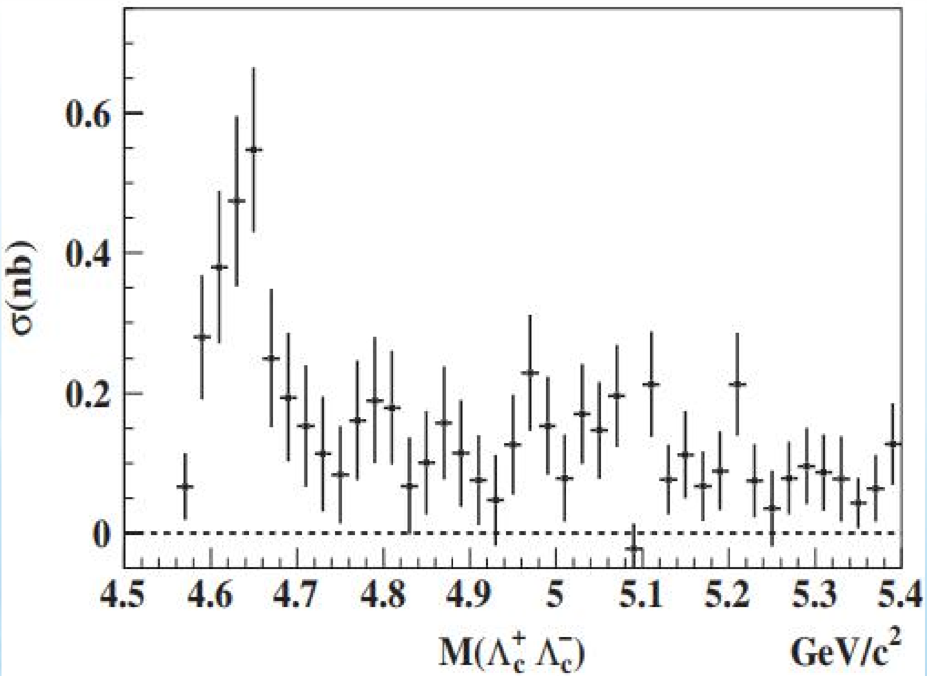

BABAR, PRD89 (2014) 111103.
Belle, PRD91 (2015) 112007,
PRL101 (2008) 172001.

Hadronic scattering amplitude

- Isospin 0, no OPE contribution
- VMD, $^3S_1$-$^3D_1$

$$
\begin{aligned}
V(^3S_1)(p',p) &= \tilde{C}_{^3S_1} + C_{^3S_1}(p'^2+p^2) - \mathrm{i}\,(\tilde{C}^a_{^3S_1} + C^a_{^3S_1}p'^2)(\tilde{C}^a_{^3S_1} + C^a_{^3S_1}p^2),\\
V(^3D_1 - {}^3S_1)(p',p) &= C_{\epsilon_1}\,p'^2 - \mathrm{i}\,C^a_{\epsilon_1}p'^2(\tilde{C}^a_{^3S_1} + C^a_{^3S_1}p^2),\\
V(^3S_1 - {}^3D_1)(p',p) &= C_{\epsilon_1}\,p^2 - \mathrm{i}\,(\tilde{C}^a_{^3S_1} + C^a_{^3S_1}p'^2)\,C^a_{\epsilon_1}p^2,\\
V(^3D_1)(p',p) &= 0\,,
\end{aligned}
$$

- One resonance exchange in ChEFT

$$
\mathcal{L} = g_V\bar{\Psi}\gamma^\mu\Psi\phi_\mu + \frac{f_V}{4M_{\Lambda_c}}\bar{\Psi}\sigma^{\mu\nu}\Psi(\partial_\mu\phi_\nu - \partial_\nu\phi_\mu) + \text{H.c.}
$$

$$
\begin{aligned}
V_{^3S_1}(p',p;E) &= \frac{4}{9m_V(E-m_V)}\left[g_V\left(1+\frac{M_{\Lambda_c}}{2E_{p'}}\right)+f_V\left(\frac{E}{4M_{\Lambda_c}}+\frac{E}{2E_{p'}}\right)\right]\left[g_V\left(1+\frac{M_{\Lambda_c}}{2E_p}\right)+f_V\left(\frac{E}{4M_{\Lambda_c}}+\frac{E}{2E_p}\right)\right]\\
V_{^3D_1}(p',p;E) &= \frac{2}{9m_V(E-m_V)}\left[g_V\left(1-\frac{M_{\Lambda_c}}{E_{p'}}\right)+f_V\left(\frac{E}{2E_{p'}}-\frac{E}{2M_{\Lambda_c}}\right)\right]\left[g_V\left(1-\frac{M_{\Lambda_c}}{E_p}\right)+f_V\left(\frac{E}{2E_p}-\frac{E}{2M_{\Lambda_c}}\right)\right]\\
V_{^3D_1-^3S_1}(p',p;E) &= \frac{2\sqrt{2}}{9m_V(E-m_V)}\left[g_V\left(1-\frac{M_{\Lambda_c}}{E_{p'}}\right)+f_V\left(\frac{E}{2E_{p'}}-\frac{E}{2M_{\Lambda_c}}\right)\right]\left[g_V\left(1+\frac{M_{\Lambda_c}}{2E_p}\right)+f_V\left(\frac{E}{4M_{\Lambda_c}}+\frac{E}{2E_p}\right)\right]\\
V_{^3S_1-^3D_1}(p',p;E) &= \frac{2\sqrt{2}}{9m_V(E-m_V)}\left[g_V\left(1+\frac{M_{\Lambda_c}}{2E_{p'}}\right)+f_V\left(\frac{E}{4M_{\Lambda_c}}+\frac{E}{2E_{p'}}\right)\right]\left[g_V\left(1-\frac{M_{\Lambda_c}}{E_p}\right)+f_V\left(\frac{E}{2E_p}-\frac{E}{2M_{\Lambda_c}}\right)\right]
\end{aligned}
$$

Born term and DWBA

- Born amplitude, including pole term and non-pole term

$$F^0_{^3S_1}(p',p;E) = -\frac{4\alpha}{9}\left\{G_{ee}\left(1+\frac{M_{\Lambda_c}}{2E_{p'}}\right)+\frac{g_{ee}}{m_V(E-m_V)}\left[g_V\left(1+\frac{M_{\Lambda_c}}{2E_{p'}}\right)+f_V\left(\frac{E}{4M_{\Lambda_c}}+\frac{E}{2E_{p'}}\right)\right]\right\}\left(1+\frac{m_e}{2E_p}\right),$$

$$F^0_{^3D_1}(p',p;E) = -\frac{2\alpha}{9}\left\{G_{ee}\left(1-\frac{M_{\Lambda_c}}{E_{p'}}\right)+\frac{g_{ee}}{m_V(E-m_V)}\left[g_V\left(1-\frac{M_{\Lambda_c}}{E_{p'}}\right)+f_V\left(\frac{E}{2E_{p'}}-\frac{E}{2M_{\Lambda_c}}\right)\right]\right\}\left(1-\frac{m_e}{E_p}\right),$$

$$F^0_{^3D_1-^3S_1}(p',p;E) = -\frac{2\sqrt{2}\alpha}{9}\left\{G_{ee}\left(1-\frac{M_{\Lambda_c}}{E_{p'}}\right)+\frac{g_{ee}}{m_V(E-m_V)}\left[g_V\left(1-\frac{M_{\Lambda_c}}{E_{p'}}\right)+f_V\left(\frac{E}{2E_{p'}}-\frac{E}{2M_{\Lambda_c}}\right)\right]\right\}\left(1+\frac{m_e}{2E_p}\right),$$

$$F^0_{^3S_1-^3D_1}(p',p;E) = -\frac{2\sqrt{2}\alpha}{9}\left\{G_{ee}\left(1+\frac{M_{\Lambda_c}}{2E_{p'}}\right)+\frac{g_{ee}}{m_V(E-m_V)}\left[g_V\left(1+\frac{M_{\Lambda_c}}{2E_{p'}}\right)+f_V\left(\frac{E}{4M_{\Lambda_c}}+\frac{E}{2E_{p'}}\right)\right]\right\}\left(1-\frac{m_e}{E_p}\right).$$

- LS and DWBA

$$T_{L''L'}(p'',p';E) = V_{L''L'}(p'',p';E) + \sum_L \int_0^\infty \frac{dpp^2}{(2\pi)^3} V_{L''L}(p'',p;E)\frac{1}{E-2E_p+i0^+}T_{LL'}(p,p';E)$$

$$F^{\Lambda_c^+\bar{\Lambda}_c^-,e^+e^-}_{L''L'}(k,k_e;E) = F^0_{L''L'}(k,k_e;E) + \sum_L \int_0^\infty \frac{dpp^2}{(2\pi)^3} T_{L''L}(k,p;E)\frac{1}{E-2E_p+i0^+}F^0_{LL'}(p,k_e;E)$$

ee→$\Lambda_c\Lambda_c$ fit

- LO $\Lambda_c\Lambda_c$ elastic scattering potential, without annihilation
- Varying the cutoffs

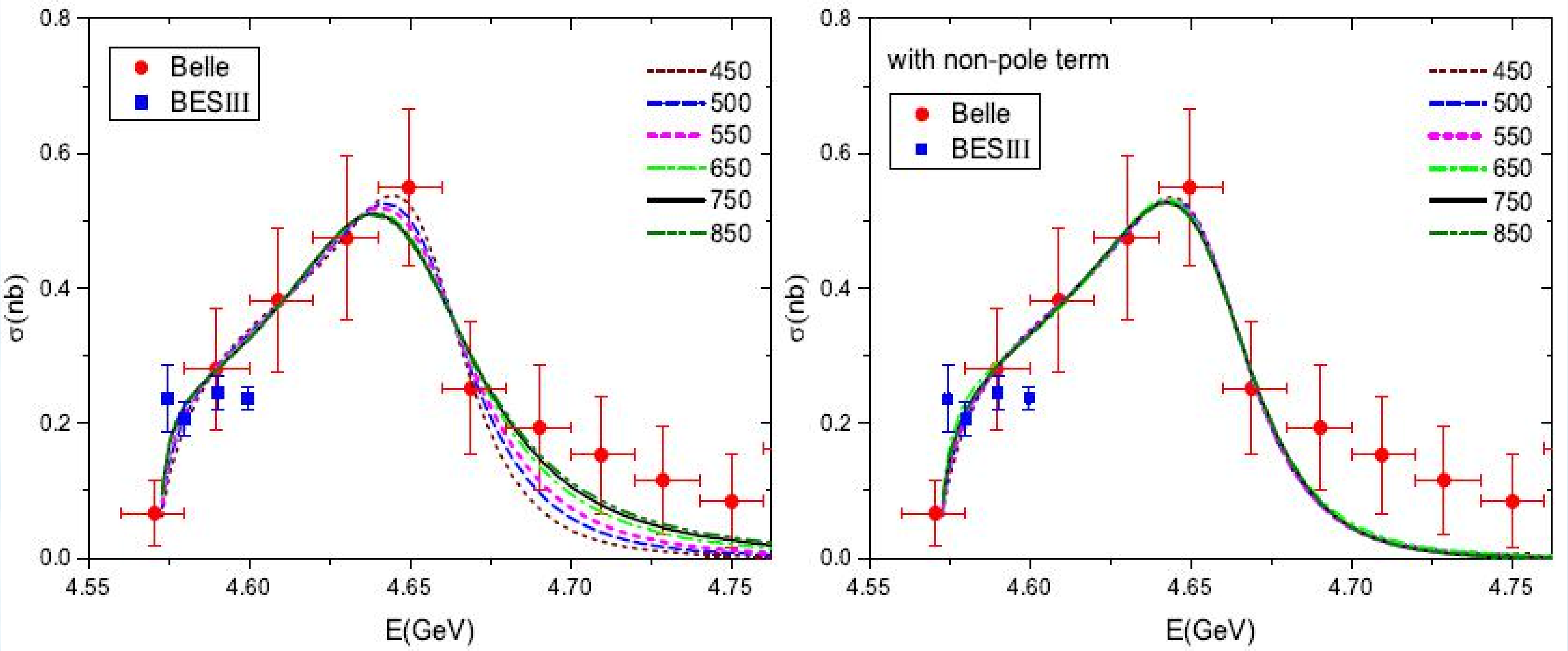

ee→$\Lambda_c\Lambda_c$ fit

- NLO $\Lambda_c\Lambda_c$ elastic scattering potential, with annihilation
- varying the number of LECs

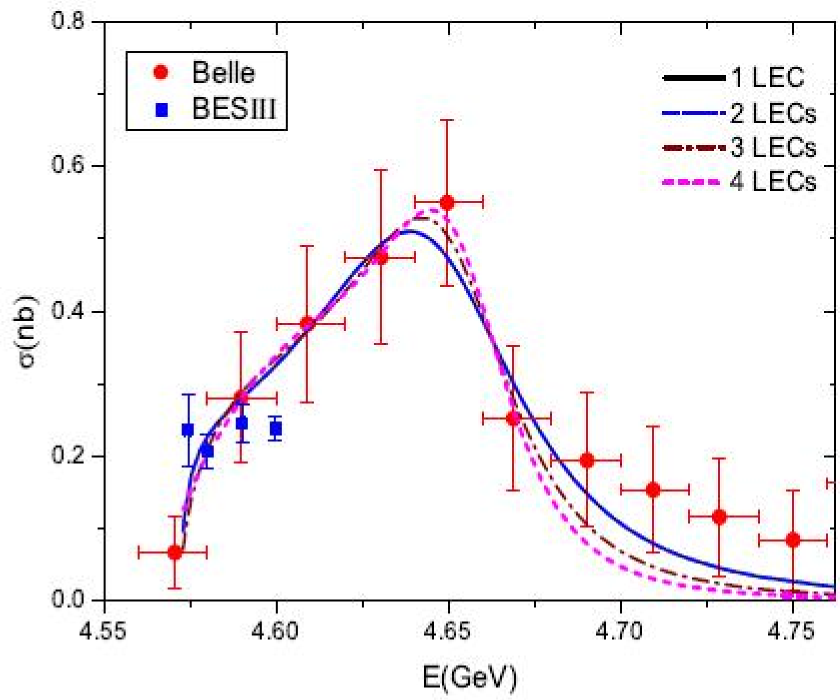

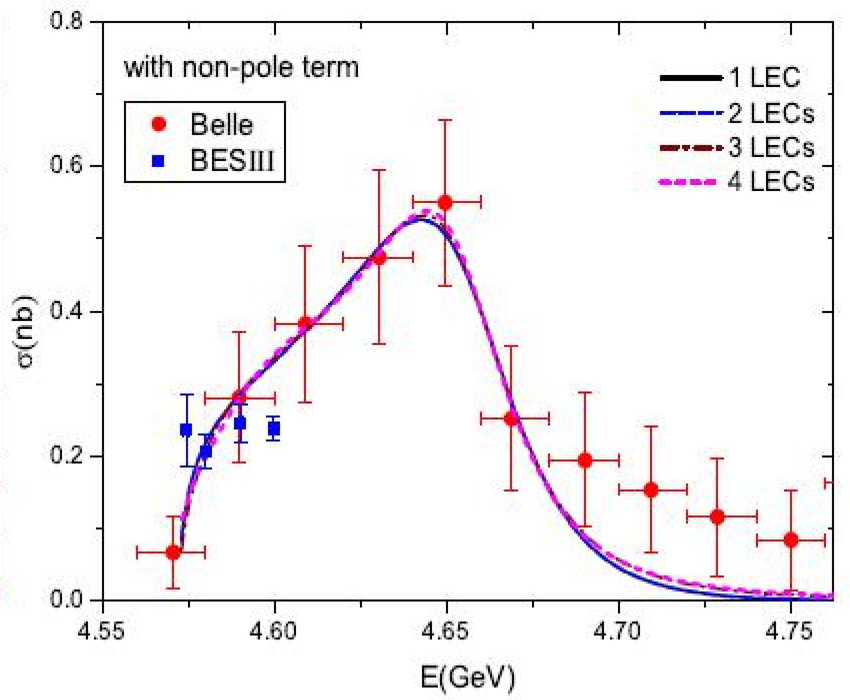

poles and scattering lengths

- Poles and scattering lengths are stable with non-pole term

Λ (GeV)	0.45	0.50	0.55	0.65	0.75	0.85
with pole term, see Eq. (4)						
$\tilde{C}_{^3S_1}$	191.8	110.1	61.27	7.853	−19.17	−34.48
g_V	−8.734	−8.123	−7.625	−6.837	−6.218	−5.706
m_V (GeV)	4.6344	4.6364	4.6383	4.6419	4.6448	4.6472
$g_{ee}(\times 10^{-3}\,\mathrm{GeV}^2)$	1.052	1.067	1.081	1.102	1.116	1.126
χ^2	0.1	0.3	0.4	0.6	0.7	0.8
pole (GeV)	4.6550	4.6534	4.6514	4.6482	4.6462	4.6451
	−i 0.0264	−i 0.0311	−i 0.0343	−i 0.0376	−i 0.0389	−i 0.0394
a (fm)	−0.269	−0.485	−0.634	−0.818	−0.927	-1.002
with pole and non-pole contribution, see Eq. (4)						
$\tilde{C}_{^3S_1}$	191.9	111.9	65.65	−0.0100	−11.76	−26.96
g_V	−8.808	−7.964	−7.356	−6.490	−5.899	−5.415
m_V (GeV)	4.6328	4.6398	4.6443	4.6473	4.6542	4.6572
$g_{ee}(\times 10^{-3}\,\mathrm{GeV}^2)$	1.055	1.052	1.042	1.045	1.004	0.987
$G_{ee}(\times 10^{-3})$	0.272	−0.578(658)	−1.035	−1.100	−1.672	−1.787
χ^2	0.1	0.1	0.2	0.2	0.2	0.2
pole (GeV)	4.6543	4.6552	4.6554	4.6532	4.6550	4.6549
	−i 0.0276	−i 0.0284	−i 0.0295	−i 0.0304	−i 0.0314	−i 0.0319
a (fm)	−0.325	−0.360	−0.403	−0.641	−0.538	−0.581

poles and scattering lengths

- Poles are not sensitive to the strength of annihilation

	1 LEC	2 LECs	3 LECs	4 LECs
with pole term.				
$\tilde{C}_{^3S_1}$ (GeV^{-2})	-19.17	-19.23	-0.1001	-49.78
$C_{^3S_1}$ (GeV^{-4})	-	-	-191.3	-146.4
$\tilde{C}^a_{^3S_1}$ (GeV^{-1})	-	0.1661	-0.5353	-1159
$C^a_{^3S_1}$ (GeV^{-3})	-	-	-	4567
g_V	-6.218	-6.218	-5.071	-4.705
m_V (GeV)	4.6448	4.6448	4.6386	4.6362
$g_{ee}(\times 10^{-3}\mathrm{GeV}^2)$	1.116	1.116	1.079	1.171
χ^2	0.7	0.7	0.3	0.1
pole (GeV)	$4.6462 - i0.0389$	$4.6455 - i0.0390$	$4.6501 - i0.0396$	$4.6506 - i0.0397$
a (fm)	-0.927	-0.928	-0.726	$-0.916 - i0.844$
with pole and non-pole contribution.				
	1 LEC	2 LECs	3 LECs	4 LECs
$\tilde{C}_{^3S_1}$ (GeV^{-2})	-11.76	-11.74	-0.0135	-60.76
$C_{^3S_1}$ (GeV^{-4})	-	-	-187.9	-74.23
$\tilde{C}^a_{^3S_1}$ (GeV^{-1})	-	0.6595	0.0503	-1185
$C^a_{^3S_1}$ (GeV^{-3})	-	-	-	5455
g_V	-5.899	-5.897	-5.012	-4.858
m_V (GeV)	4.6542	4.6542	4.6414	4.6342
$g_{ee}(\times 10^{-3}\mathrm{GeV}^2)$	1.004	1.003	1.063	1.200
$G_{ee}(\times 10^{-3})$	-1.672	-1.679	-0.455	0.512
χ^2	0.2	0.2	0.2	0.1
pole (GeV)	$4.6550 - i0.0314$	$4.6546 - i0.0312$	$4.6520 - i0.0285$	$4.6482 - i0.0341$
a (fm)	[illegible]	[illegible]	[illegible]	$-0.981 - i0.714$

	present analysis	Belle [8]	Belle [7]	BABAR [6]
reaction	$e^+e^- \to \Lambda_c^+\bar{\Lambda}_c^-$	$e^+e^- \to \Lambda_c^+\bar{\Lambda}_c^-$	$e^+e^- \to \pi^+\pi^-\psi(2S)$	$e^+e^- \to \pi^+\pi^-\psi(2S)$
mass M (MeV)	$4652.5 \pm 3.4 \pm 1.1$	$4634^{+8}_{-7}{}^{+5}_{-8}$	$4652 \pm 10 \pm 8$	$4669 \pm 21 \pm 3$
width Γ (MeV)	$62.6 \pm 5.6 \pm 4.3$	$92^{+40}_{-24}{}^{+10}_{-21}$	$68 \pm 11 \pm 1$	$104 \pm 48 \pm 10$

Electromagnetic formfactor

- Effective form factors for LO, NLO
- BESIII's has a different trend comparing to Belle's
- The future measurement of BESIII up to 4.65 GeV is important

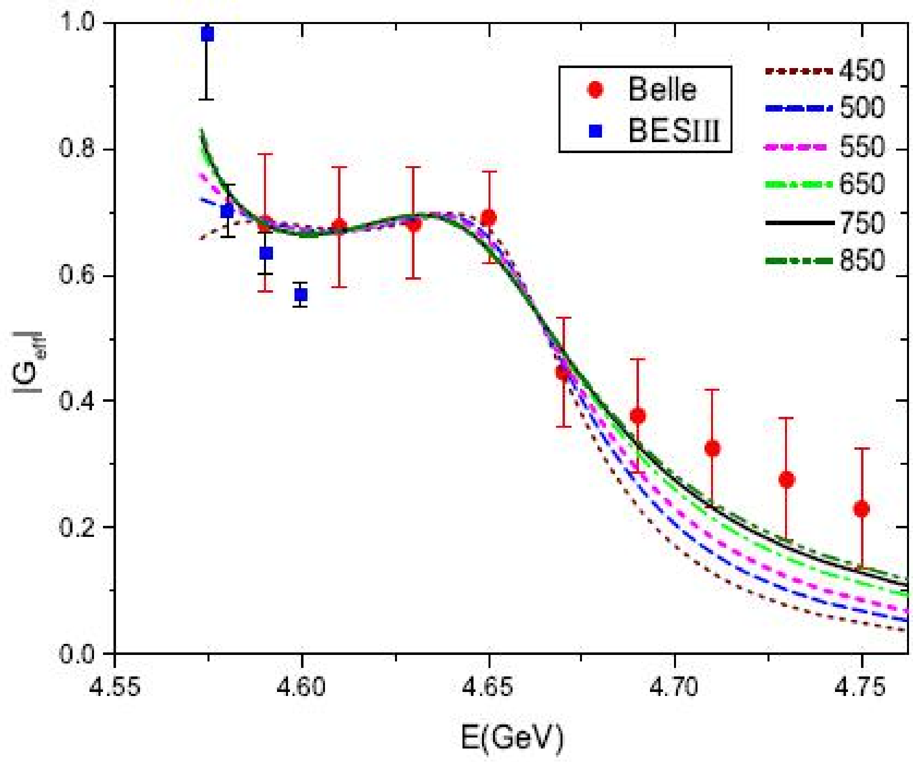

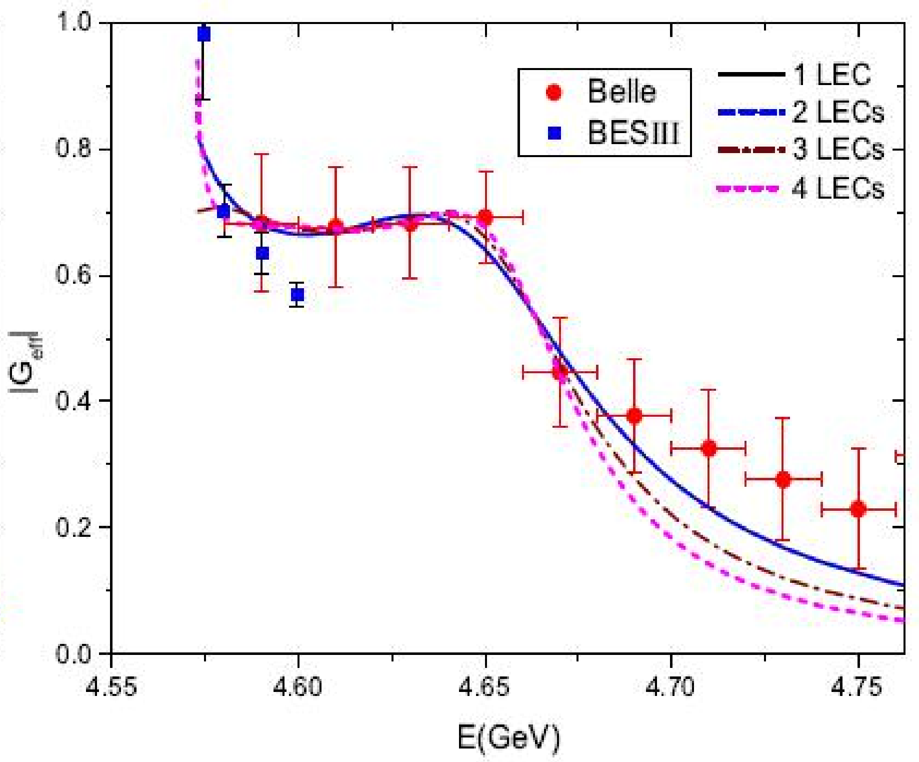

6. Summary

NN Amplitude

Up to N^{3}LO, we fit ChEFT amplitude to PWA's. It works well at PLab<300 MeV for S- and P-waves, and a bit lower for higher partial waves. Its low energy part is also consistent with the antiprotonic hydrogen phenomenology.

NN

We are studying the proton FF from ee →pp up to N3LO, with LS equation and DWBA method. The structure around pp threshold exhibits a cusp-like behavior.

$\Lambda_c\Lambda_c$

We study e+e− →$\Lambda_c\Lambda_c$ process close to the theshold. the pole location of X(4630/4660) is obtained.The Λ_c FF is predicted.

Prospects

Amplitude analysis, analytical continuation to obtain the FF in unphysical region?

Thank You For your patience !